

29

PL-TR-93-2043
Environmental Research Papers, No. 1121

AD-A279 399



A MODEL FOR C_n^2 (OPTICAL TURBULENCE) PROFILES USING RADIOSONDE DATA

E. M. Dewan
R. E. Good
R. Beland
J. Brown

DTIC
ELECTE
MAY 02 1994
S G D

1 March 1993

Approved for public release; distribution unlimited

UNCLASSIFIED

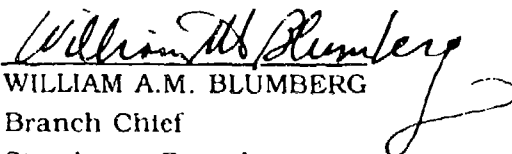
94-12991
55491



PHILLIPS LABORATORY
Directorate of Geophysics
AIR FORCE MATERIEL COMMAND
HANSCOM AIR FORCE BASE, MA 01731-3010

94 4 28 051

"This technical report has been reviewed and is approved for publication"


WILLIAM A.M. BLUMBERG
Branch Chief
Simulation Branch
Optical Environment Division


ROGER A. VAN TASSEL
Division Director
Optical Environment Division

This document has been reviewed by the ESD Public Affairs Office (PA) and is releasable to the National Technical Information Service (NTIS).

Qualified requestors may obtain additional copies from the Defense Technical Information Center. All other should apply to the National Technical Information Service.

If your address has changed, or if you wish to be removed from the mailing list, or if the addressee is no longer employed by your organization, please notify PL/TSI, Hanscom AFB, MA 01731-3010. This will assist us in maintaining a current mailing list.

Do not return copies of this report unless contractual obligations or notices on a specific document requires that it be returned.

REPORT DOCUMENTATION PAGE

Form Approved
OMB No. 0704-0188

Public reporting burden for this collection of information is estimated to average 1 hour per response, including the time for reviewing instructions, searching existing data sources, gathering and maintaining the data needed, and completing and reviewing the collection of information. Send comments regarding this burden estimate or any other aspect of this collection of information, including suggestions for reducing this burden, to Washington Headquarters Services, Directorate for Information Operations and Reports, 1215 Jefferson Davis Highway, Suite 1204, Arlington, VA 22202-4302, and to the Office of Management and Budget, Paperwork Reduction Project (0704-0188), Washington, DC 20503

1. AGENCY USE ONLY (Leave blank)	2. REPORT DATE 1 March 1993	3. REPORT TYPE AND DATES COVERED Scientific Interim	
4. TITLE AND SUBTITLE A MODEL FOR C_n^2 (OPTICAL TURBULENCE) PROFILES USING RADIOSONDE DATA		5. FUNDING NUMBERS PE: 61102F PR 2310 TA G5 WU 04	
6. AUTHOR(S) E. M. Dewan, R. E. Good, R. Beland and J. Brown			
7. PERFORMING ORGANIZATION NAME(S) AND ADDRESS(ES) Phillips Laboratory (GPOS) 29 Randolph Road Hanscom AFB, MA 01731-3010		8. PERFORMING ORGANIZATION REPORT NUMBER PL-TR-93-2043 ERF, No. 1121	
9. SPONSORING / MONITORING AGENCY NAME(S) AND ADDRESS(ES)		10. SPONSORING / MONITORING AGENCY REPORT NUMBER	
11. SUPPLEMENTARY NOTES			
12a. DISTRIBUTION / AVAILABILITY STATEMENT Approved for public release; distribution unlimited		12b. DISTRIBUTION CODE	
13. ABSTRACT (Maximum 200 words) The structure constant, C_n^2 , for optical index of refraction fluctuations is the key to the design of adaptive optical systems that minimize the effects of turbulence on laser beam propagation. This report explains our model, which converts standard radiosonde data into C_n^2 profiles. The results are compared to directly measured <i>in situ</i> values of C_n^2 obtained by means of balloon borne thermosondes. The AFGL model is also compared to two other such radiosonde models, and we describe the results from three test programs.			
14. SUBJECT TERMS Transmission, Optical turbulence, Laser beam propagation, Turbulence, Radiosondes, Atmospheric turbulence		15. NUMBER OF PAGES 52	16. PRICE CODE
17. SECURITY CLASSIFICATION OF REPORT UNCLASSIFIED	18. SECURITY CLASSIFICATION OF THIS PAGE UNCLASSIFIED	19. SECURITY CLASSIFICATION OF ABSTRACT UNCLASSIFIED	20. LIMITATION OF ABSTRACT SAR

Accession For	
NTIS CRA&I	<input checked="" type="checkbox"/>
DTIC TAB	<input type="checkbox"/>
Unannounced	<input type="checkbox"/>
Justification	
By	
Distribution/	
Availability Codes	
Dist	Avail and/or Special
A-1	

Contents

1. INTRODUCTION	1
2. THE AFGL RADIOSONDE MODEL FOR C_n^2 (ABOVE THE BOUNDARY LAYER)	2
2.1 Basic Concepts	3
2.2 The Small Scale L - Model	3
2.3 Model Application to Radiosonde Data	8
3. MODEL TESTS	8
4. COMPARISONS: CLEAR-1 DATA	9
5. COMPARISONS, HAWAIIAN PROGRAM 1984 DATA	17
6. COMMENTS AND SUGGESTIONS FOR FUTURE WORK	28
7. CONCLUSIONS	29
REFERENCES	30
APPENDIX A: MODELING C_n^2 PROFILES FROM RADIOSONDE DATA	31
APPENDIX B: SHEAR REGRESSIONS	41

Illustrations

1	Illustration of how turbulent layers are determined	4
2	Plot of $Y = \log \langle (L_1)^{4/3} \rangle$ vs S_{raw} on log-linear graph, for the troposphere.	5
3	Plot of $Y = \log \langle (L_1)^{4/3} \rangle$ vs S_{raw} on a log-linear graph, for the stratosphere.	6
4	Comparisons between the Thermosonde Derived Profiles and A) the AFGL Model; B) the Van Zandt (NOAA) Model; and C) the Hufnagel model for Flight No. 1 of the CLEAR-1 Program.	13
5	Comparisons between the Thermosonde Derived Profiles and A) the AFGL Model; B) the Van Zandt (NOAA) Model; and C) the Hufnagel model for Flight No. 4 of the CLEAR-1 Program.	14
6	Comparisons between the Thermosonde Derived Profiles and A) the AFGL Model; B) the Van Zandt (NOAA) Model; and C) the Hufnagel model for Flight No. 10 of the CLEAR-1 Program.	15
7	Plot of $Y = \log \langle (L_1)^{4/3} \rangle$ vs S_{raw} on a log-linear graph, for the Tropospheric Alternate Model.	16
8	Radiosonde Measurements for Flight No. 5 of the Hawaiian Campaign (1984).	18
9	Model and Thermosonde Profile Comparisons for Flight 01 of the Hawaiian Campaign (1984).	23
10	Model and Thermosonde Profile Comparisons for Flight 49 of the Hawaiian Campaign (1984) in the same format as in Figure 9.	25

List of Tables

1.	Clear-1 Flights	9
2.	Isoplanatic Angle Figures of Merit " $Z^{5/3}$ "	10
3.	Scintillation Variance " $Z^{5/6}$ "	10
4.	Percentage Error Comparisons for Isoplanatic Angle $[(\text{Model} - \text{Exper.})/\text{Exper.}] \times 100$	11
5.	Isoplanatic Angle Figures of Merit From Alternative Model " $Z^{5/3}$ "	12
6.	Scintillation Variance Figures of Merit From Alternative Model " $Z^{5/6}$ "	12
7.	Isoplanatic Angle Figures of Merit for the 1984 Hawaiian Program Data $(Z^{5/3})^{3/5}$	27
8.	Scintillation Variance Figures of Merit for the 1984 Hawaiian Program Data $(Z^{5/6})$	27
A1.	Values of $I \times 10^7$ for Various Radiosonde Models and for Thermosonde Measurements in the Altitude Range of 5 km to z max	36
A2.	Values of θ_0 for Various Radiosonde Models and Thermosonde Measurements	36
A3.	Comparison Between AFGL and VanZandt Models	37
B1.	Alternative Models	41

Acknowledgements

We acknowledge help from Edmund Murphy and Carol Bevis for typing this manuscript under trying circumstances. The principal author thanks AFOSR, under Project SOAR, for sponsoring the final phase of the work.

Caveats

The model described in this report was originally intended for use in connection with nearly vertical laser beam propagation (ground to space and vice versa). For this reason the verification was based on such trajectories and therefore this model has not been tested for horizontal or nearly horizontal propagation.

The geometry of atmospheric turbulence has been described in the literature as being like "horizontal pancakes". The layers of turbulence are thin in the vertical and very large in the horizontal. This means that the case for nearly horizontal beam propagation is very different from the nearly vertical case. The C_n^2 values change rapidly and wildly in the vertical direction and can be almost uniform horizontally over the distance of kilometers. What is required is validation for horizontal trajectories, and the latter has yet to be done.

There is yet another point to be made. The present model presumes that the beam is nearly perpendicular to the "turbulent pancake layers". What happens when the beam is nearly parallel? It is possible that it could, for example, reflect from sharp discontinuities of index of refraction at layer boundaries. This and other such effects are not included in the *physics* of the present model. This may have to be investigated also before one has a valid approach to the case of nearly horizontal beams. At the very least some theoretical justification would have to be given for ignoring these omissions.

A Model for C_n^2 (Optical Turbulence) Profiles Using Radiosonde Data

1. Introduction

Currently, models are needed to convert standard meteorological data into vertical profiles of C_n^2 , the structure constant for optical index of refraction fluctuations. For background information see Tatarski,¹ (1961), and Dewan² (1980). The latter report contains many other references. Profiles of C_n^2 from the ground to 20 or 30 km are needed to ascertain the effects of turbulence on laser beam propagation from ground to space as well as on light propagation from space to ground. Such information would be available in large quantities if radiosonde information could be converted to C_n^2 profiles. Such information could then be used for assigning design parameters for adaptive optical systems, which can greatly reduce the effect of turbulence.

This report† describes our radiosonde C_n^2 model* and tests of it. Note that this model does not relate to the convective boundary layer and our tests will be applied with this in mind. Other models exist for the boundary layer and these would be added, for example, when parameters such as r_0 , the coherence length, are estimated, because r_0 is sensitive to near-ground C_n^2 . In this report we will only consider parameters sensitive to C_n^2 above the boundary layer.

This report describes how the AFGL model was created from very high resolution velocity profiles that we obtained in the stratosphere by means of rocket laid smoke trails; next it will explain how the resulting model is used to convert radiosonde data into C_n^2 profiles. Then, comparisons between model and thermosonde profiles of C_n^2 will be made. In addition, the AFGL model will be compared to two other radiosonde models, namely, those due to Hufnagel³ (HUF) and to VanZandt⁴ (VZ). Three field programs will be discussed, namely, CLEAR-1, and Hawaii (1984) in the main text, and CLEAR-3 in Appendix 1.

At the end of the report some comments will be made about the lessons we learned in this research. Suggestions for future research will also be offered. Appendix A contains a paper that describes the VZ and HUF models and additional model comparisons, and Appendix B contains more information on high resolution shear regressions.

Received for publication 26 Feb 1993

† The original draft of this manuscript originated 25 Feb 1987.

* Hereafter this will be denoted the AFGL model, for reasons of established conventions in the literature.

2. The AFGL Radiosonde Model for C_n^2 (Above Boundary Layer)

2.1 Basic Concepts

The key equation for the AFGL model is:

$$C_n^2 = 2.8 M^2 L^{4/3} \quad (1)$$

where:

$$M^2 = \left[\left(\frac{79 \times 10^{-6} P}{T^2} \right) \left(\frac{dT}{dz} + \gamma \right) \right]^2 \quad (2)$$

and where T is absolute atmospheric temperature in $^{\circ}\text{K}$, P is pressure in mb, γ is the dry adiabatic lapse rate of $9.8 \times 10^{-3} \text{ }^{\circ}\text{K/m}$, and z is the height above ground. (Tatarski, 1961, and Dewan, 1980). Radiosondes give us P and T directly, but L in Eq. (1) is "the outer length," that is, the largest scale of inertial range turbulence. This is the unknown that our model will supply. A good rule of thumb, based on information in Pond et al (1963) and Tennekes and Lumley (1972), is that L would be of the order of 0.1 times the thickness of a turbulent layer. In principle this could be used in the future as an adjustable parameter (that is, one could use values other than 0.1) but at present using other values seems to be unnecessary.

We now consider the question "How can one estimate L from radiosonde data?" which will occupy us until Section 2.3. It is generally known that above the convective boundary layer, atmospheric turbulence occurs in thin layers shaped like pancakes that are miles in width and tens of meters thick (usually). A shear type of instability leads to the formation of the layers, and the shears are generally caused by gravity waves (Dewan and Good, 1986).⁷ We used the common rule of thumb

$$Ri \equiv N^2 / S^2 < 0.25 \quad (3)$$

where Ri is the Richardson number, N is the buoyancy frequency, and S is the vector vertical shear of the horizontal velocity defined as

$$S \equiv \left[\left(\frac{dV_N}{dz} \right)^2 + \left(\frac{dV_E}{dz} \right)^2 \right]^{1/2} \quad (4)$$

where V_N and V_E are the north and east horizontal wind components. In a paper as yet unpublished, by Dewan and Good, we found that data supported the instability criterion

$$(S_c)^2 > (N)^2 (0.5)^{-1} \quad (5)$$

and, in the present report we shall use Eq. (5).

Standard radiosondes report data, such as velocity, at intervals of 300 m and larger. When such velocities are used in Eq. (4), only rarely will condition (5) hold. Presumably, since one

expects that the layers are of order 1/10 the resolution of the radiosondes, the shears responsible must be on that same scale. Van Zandt et al. (1981)⁴ pointed this out and indicated the resultant need for a statistical model to estimate small scale wind structure. We must use a statistical association between the large scale shears, called S_{raw} here (that are measured by radiosondes) and the average of $L^{4/3}$ contained within the 300 m height range, which are based on the small scale but unmeasurable shears.

2.2 The Small Scale L-Model

To obtain the statistical association mentioned above we used our high resolution (10 m) stratospheric velocity profiles described in Dewan et al. (1984).⁸ In all, these data consisted of 55.3 km of velocity profile information. The choice of 300 m for "radiosonde scale", is not as arbitrary as might appear. It is based in part on subsequent model performance.

Our procedure is described with reference to Figure 1. The first step is to obtain the high resolution shears (from the previously mentioned 10 m winds) as a function of z by using Eq. (4). Using Eq. (5) and the US Standard Atmosphere we found that $S_c = 0.015 \text{ s}^{-1}$ for the troposphere and 0.03 s^{-1} for the stratosphere. Next, all shear regions exceeding S_c are presumed turbulent. As shown in Figure 1, turbulent layer thicknesses, \mathcal{L}_i are assigned to these regions. We will use:

$$L_i = 1/10 \mathcal{L}_i \quad (6)$$

but the 1/10 factor is not taken into account until the model is actually applied to the radiosonde data.

Next, we obtained a weighted average of $(\mathcal{L}_i)^{4/3}$ from

$$\langle \mathcal{L}_i^{4/3} \rangle \equiv \sum \mathcal{L}_i^{4/3} (\mathcal{L}_i / 290) \quad (7)$$

Occasionally a layer L_i will protrude outside of the 300 m region of interest. In such a case the \mathcal{L}_i in the term $(\mathcal{L}_i / 290)$ of Eq. (7) is reduced to include only the amount of \mathcal{L}_i within the 300 m region.

Several methods to obtain S_{raw} are described in Appendix B; however, in the model of choice, (on the basis of performance) we first smoothed the velocities with an 11 point running average and then differences the velocities across the 300 m region and divided the result by 300 m. This gave us S_{raw} . Finally we plotted $\langle \mathcal{L}_i^{4/3} \rangle$ against S_{raw} in Figures 2 and 3 on a log-linear plot and obtained a straight line regression in these coordinates. The maximum raw shear used in the regression was 0.045 s^{-1} . The resulting models are:

$$\begin{aligned} \log \langle \mathcal{L}_i^{4/3} \rangle &\equiv Y = 1.64 + 42.0 S_{raw} && \text{(Troposphere)} \\ Y &= 0.506 + 50.0 S_{raw} && \text{(Stratosphere)} \end{aligned} \quad (8)$$

This is to be used in Eq. (10) below.

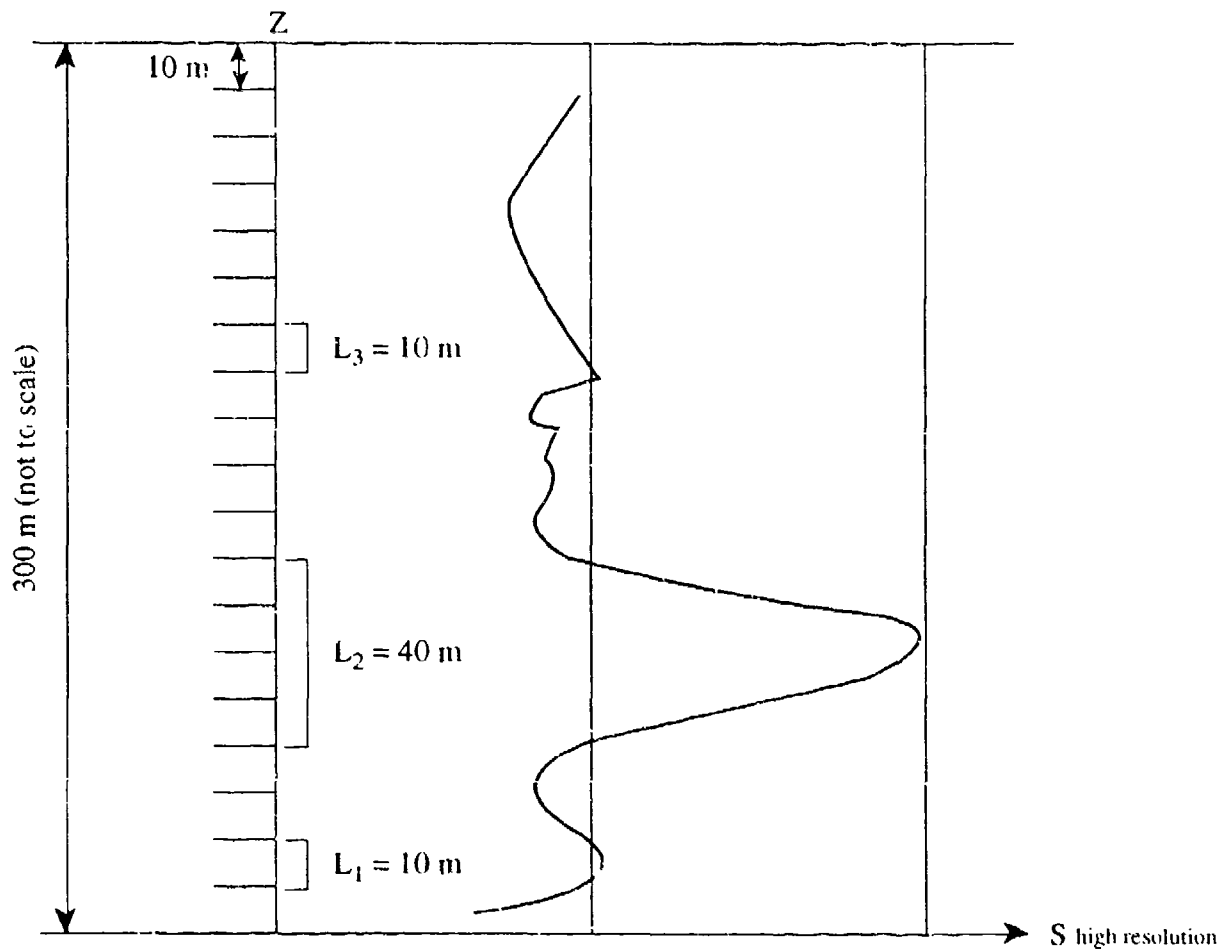


Figure 1 — Method for assigning S_{raw} to $\langle L^{4/3} \rangle$.
 (Uses weighted average, Eq (7).)

TROPOSPHERE

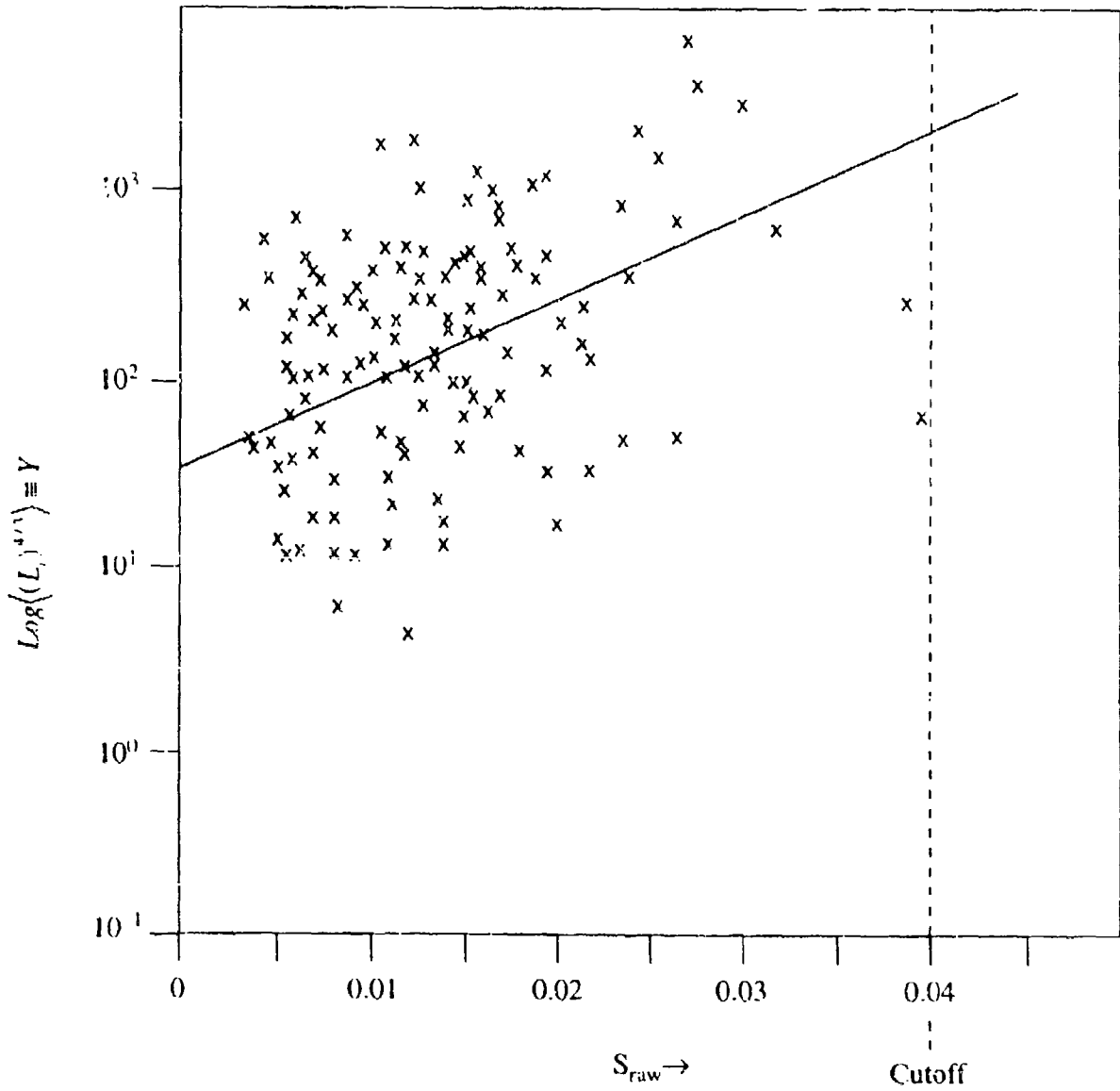


Figure 2 — 10^Y vs S_{raw} Regression. This is the Regression for the Tropospheric Model ($S_c = 0.015$).

STRATOSPHERE

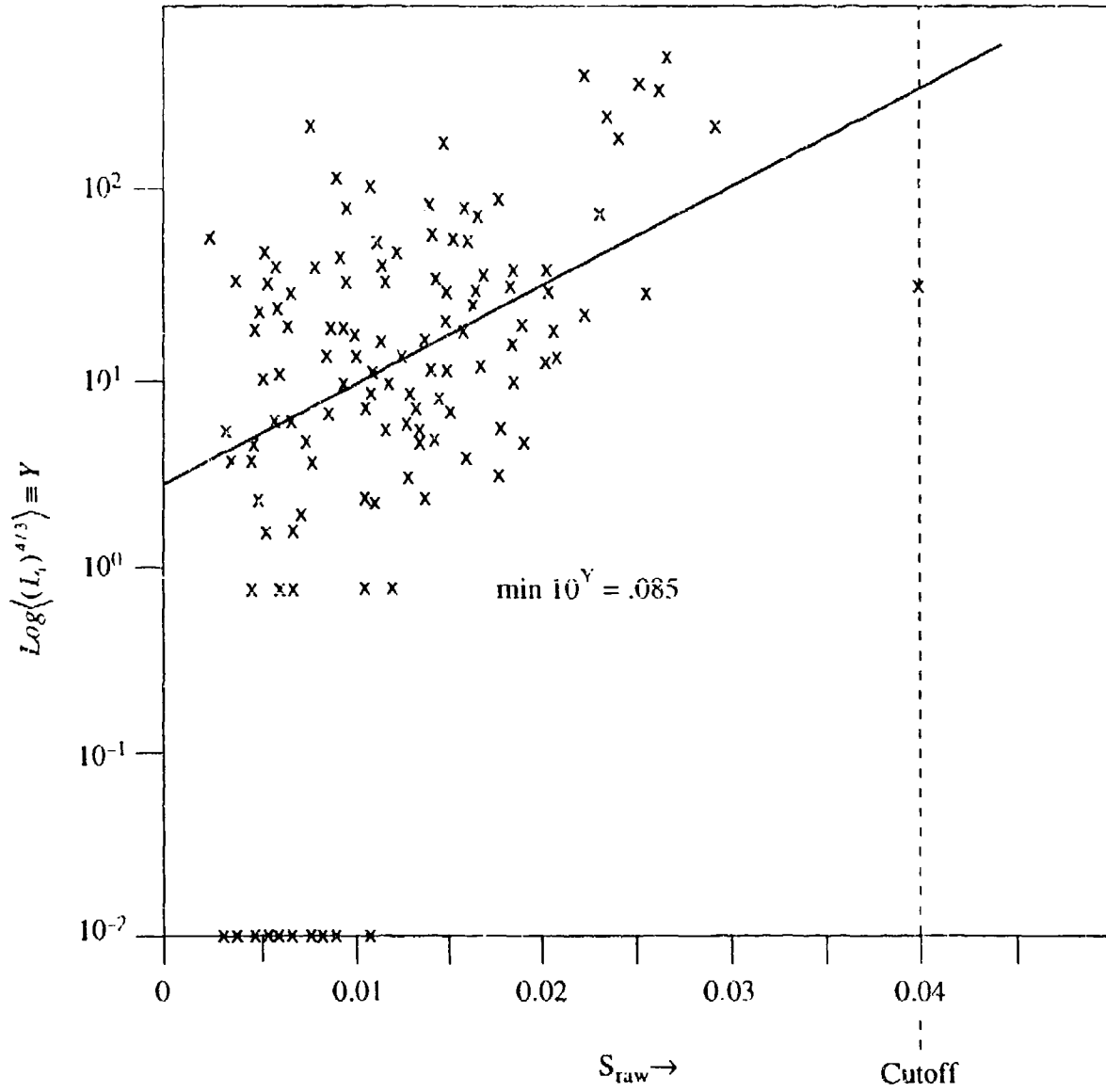


Figure 3 — Regression for the Stratospheric Model ($S_c = 0.03$).

These regressions were obtained from data analyzed for every 10 m (that is, the 300 m region was shifted by 10 m for each output pair of $\langle L_1^{4/3} \rangle$ and S_{raw}). It is clear that the number of independent points was 1/30 of the total number of points (the latter being of order 4,000). For this reason only every 30th point is exhibited in Figures 2 and 3. Taking this into account, we estimated (slightly overestimated) the standard deviations for the regressions as:

$$\begin{aligned}\sigma_{slope} &= 6.9 \\ \sigma_{const} &= 6 \times 10^{-2}\end{aligned}$$

These are based on (Bevington (1969))

$$\begin{aligned}\sigma_{fit}^2 &= [1/(N-2)] \sum (y_i - a - bx_i)^2 \\ \sigma_{slope}^2 &= \sigma_{fit}^2 / \sum (x_i)^2 \\ \sigma_{const}^2 &= \sigma_{fit}^2 / N\end{aligned}$$

Using a representative value of $S_{raw} = 0.02 \text{ s}^{-1}$ we estimate that the spread in the measurements introduces an uncertainty of about a factor of 1.6 in C_n^2 . Generally such a spread is unsatisfactory; but since C_n^2 can vary over a range of several orders of magnitude, a factor of 1.6 is considered to be essentially negligible.*

Figures 2 and 3 show a large scatter of data points about the lines. In spite of this we will see that the model performs well. The explanation lies in the fact that the standard deviation of a linear regression is like that of a mean quantity: an additional factor of the square root of a number of independent cases is involved in the "standard error" of the mean.

While Eq. (8) is the model of choice, a slightly different model was employed below, namely:

$$\begin{aligned}\text{troposphere } Y &= 1.57 + 40.0 S_{raw} \\ \text{stratosphere } Y &= 0.503 + 51.2 S_{raw}\end{aligned}\tag{9}$$

but the difference is not important to model performance.

An additional point must be made regarding the application of our model to the troposphere. As has been mentioned, all of the velocities in our statistical data base are from the stratosphere. For this reason we must assume that this data base does not differ significantly in shear statistics from actual tropospheric statistical characteristics.*

* (If $S_{raw} = 0.04 \text{ s}^{-1}$, the uncertainty in C_n^2 or 10^Y (due to the $\sigma_{const} = 0.06$ and $\sigma_{slope} = 6.9$) increases to a factor of about 2.2. $S_{raw} = 0.04 \text{ s}^{-1}$ is very rarely seen.)

+ (This assumption is weak, and if future experiments were to show that the tropospheric model is inferior to the stratospheric model, it is precisely here that one should start to look. As shown in Dewan and Good [1986] the velocity spectra are significantly different in the troposphere as compared to the stratosphere.)

2.3 Model Application To Radiosonde Data

Our model consists essentially of Eq. (1). Equation (2) is evaluated directly from raw radiosonde information. When we used high resolution pressure and temperature sensors, we preprocessed the data in a manner to be described. Using Eq. (4), the velocity information was converted into shears, which were then inserted into Eq. (9) to obtain $Y \equiv \log_{10} \langle \mathcal{L}^{4/3} \rangle$. Finally, the $C_n^2(z)$ profile was obtained from:

$$C_n^2(z) = 2.8 (0.1)^{4/3} M^2 10^Y \quad (10)$$

where the factor (0.1) comes from Eq. (6). Note that Eq. (9) contains in effect two independent pieces of the model that are applied to the stratosphere and troposphere separately. Thus, to apply this AFGL model one must first ascertain the altitude of the tropopause. In all the cases we studied this was unambiguous; but this may or may not be a problem when the model is applied to a larger volume of data, since tropopause height can be ambiguous, as is known from published data. In connecting the tropospheric model to the stratospheric model we used linear interpolation. Finally, it should be mentioned that it was necessary to build certain upper limits into the model. If the raw shear is greater than 0.04, the model assigns the value 0.04 to the shear. This was necessary because a single outlier shear due to an artifact could totally dominate the effects of the entire C_n^2 profile.

Similarly, we also placed an upper limit on dT/dz in the tropospheric model. We never allowed it to exceed zero and all gradients which did were set equal to 10^{-3} . The stratospheric model would most likely require a positive upper limit on the temperature gradient but this is left to future research because raw radiosonde information in that region was limited when this report was written.

3. Model Tests

As was mentioned in the introduction, we compared the model C_n^2 profiles to both experimental profiles and to the profiles generated by the VanZandt⁴ and Hufnagel³ models. These latter models are described in Appendix A. To parameterize the relative performance of these models, we constructed two "figures of merit" based upon two crucial adaptive optical parameters. These were the isoplanatic angle, θ_0^2 ,* and the variance due to scintillation, σ_x^2 . These are obtained from:

$$\theta_{0(rad)} = \left\{ 2.91 k^2 \int_{z_1}^{z_2} C_n^2(z) (z)^{5/3} dz \right\}^{-1/5} \quad (11)$$

* θ_0 is the angle over which the wave front correction (in an adaptive optics system) is essentially homogeneous. In other words, it is the field angle over which the optical transfer function is constant.

where k is the optical wave number $\cong 2\pi/\lambda$, and

$$\sigma_{\lambda}^2 \cong \langle \ln(A/A_0)^2 \rangle = 0.56k^{7/6} \int C_n^2(z)(z)^{5/6} dz \quad (12)$$

We thus use, for figures of merit,

$$Z^{5/3} \cong \int_{5km}^{z_{max}} C_n^2(z)(z)^{5/3} dz \quad (13)$$

and

$$Z^{5/6} \cong \int_{5km}^{z_{max}} C_n^2(z)(z)^{5/6} dz \quad (14)$$

The lower limits on these integrals were chosen to avoid the boundary layer, and all altitudes, z , are distances above ground as opposed to "above sea level".

4. Comparisons: Clear-1 Data

During the CLEAR-1 program we obtained data from 49 thermosonde flights. To compare results from standard radiosondes we used the routine meteorological flights from El Paso located about 50 miles from the thermosonde launch site. Only those thermosonde flights nearest in time to radiosonde launches were used in our comparisons. Table 1 lists the flight information. Figures 4, 5, and 6 show examples of the profiles. Tables 2 and 3 list the figure of merit comparisons, and Table 4 gives the percentage error comparisons of $Z^{5/3}$.

Table 1. CLEAR-1 Flights

Flight Number	1984 Date	Launch, PM Thermosonde Serial No.	El Paso Thermosonde Time (Local, S.T.)	Radiosonde Local S.T.	Altitude Ranges (km)
1	9/4	0508	1:48	5:00	5.3 - 15.3
2	9/5	0506	1:05	5:00	6.0 - 15.3
3	9/6	1885	2:05	5:00	5.7 - 15.3
4	9/7	1882	2:17	5:00	6.1 - 15.2
5	9/8	0524	1:43	5:00	5.8 - 15.3
6	9/10	1878	5:40	5:00	6.1 - 15.1
7	9/11	1889	8:03	5:00	8.8 - 15.2
8	9/13	2703	2:01	5:00	5.9 - 15.3
9	9/16	2757	7:51	5:00	5.2 - 15.2
10	9/18	2769	1:53	5:00	5.3 - 15.4
11	9/24	2762	8:08	5:00	5.2 - 15.2
			(Launch)		(TROPO.)

Table 2. Isoplanatic Angle Figures of Merit " $Z^{5/3}$ "

Flight Number	Radiosonde Models " $Z^{5/3}$ " x 10^7 †			Thermosonde $Z^{5/3}$ x 10^7 (Experiment)
	AFGL	HUF	VZ	
1	3.93*	1.84	3.35	4.50
2	8.27*	1.30	3.52	10.9
3	4.63	1.49	3.40*	3.81
4	7.83	3.36*	13.0	2.67
5	7.12	2.80*	5.92	3.76
6	6.62 (71)**	1.09	2.25*	2.29
7	4.46	0.618	2.39*	2.42
8	4.84 (6)**	1.25	2.42*	2.45
9	4.43*	0.665	2.72	5.05
10	7.13	0.860	3.83*	4.79
11	7.50 (9)**	4.93*	5.42	2.03
TOTAL	3	3	5	

* = closest model

† MODEL: $1.566 + 40.03 S_{raw}$ (TROPO. almost exclusively) $0.5033 + 51.32 S_{raw}$ (STRAT.) Only two significant figures are really involved here, as well as in all the other tables below. These two models are in reference to Eq. (8) for Y.

** All numbers in these tables in parentheses are based on the unsaturated model when this differs from the saturated model. Note that they occasionally are "wild," thus the need for saturation.

‡ This means that $Z^{5/3}$ is first multiplied by 10^7 and the result is entered into the table.

Table 3. Scintillation Variance Figures of Merit " $Z^{5/6}$ "

Flight Number	Radiosonde Models " $Z^{5/6}$ " x 10^{10}			Thermosonde " $Z^{5/6}$ " x 10^{10} (Experiment)
	AFGL	HUF	VZ	
1	1.77*	0.857	1.71	1.78
2	4.25*	0.595	1.73	4.10
3	2.41 (3)	0.688	1.84*	1.73
4	3.14	1.48*	5.63	1.14
5	2.8	1.25*	2.82	1.57
6	2.70 (30)	0.502	1.05*	1.08
7	1.64	0.252	0.982*	0.918
8	2.42	0.575	1.20*	0.986
9	2.05*	0.348	1.33	2.36
10	3.38	0.432	1.85*	2.35
11	3.70	2.21*	2.73	0.773
TOTAL	3	3	5	

* = closest model

MODEL: $1.566 + 40.03 S_{raw}$ (TROPO. almost exclusively) $0.503 + 51.32 S_{raw}$ (STRAT.)

Table 4. Percentage Error Comparisons for Isoplanatic Angle
{(Model - Exper.) / Exper.} × 100%

Flight Number	AFGL	HUF	VZ	(Z ^{5/3} ONLY)
1	-13	-59	-25	
2	-24	-88	-67	
3	22	-60.9	10.8	
4	193	25.8	386	
5	89	-25.5	57.5	
6	189	-52.4	-1.75	
7	84	-74	-1.24	
8	98	-49	-1.22	
9	-12.3	-86	-46	
10	49	-82	-20	
11	269	142	160	

Up until this point our conclusions (based on Tables 1-4) are that (a) the VanZandt model gave the closest values to the thermosonde the largest number of times, and (b) it also came the closest in value if one eliminates the two worst cases in all of them.

Tables 2 - 4 were supplemented by Tables 5 and 6, which used an alternative model as indicated. Despite the large apparent difference in these regressions, as seen in Figures 2 and 3 in comparison to Figure 7 and in the models, as indicated explicitly in the tables, the results were hardly affected, and the relative scores of the models did not change. Figure 7 shows the alternative tropospheric model (the one used almost exclusively in the sense that the stratospheric model was not used significantly, since CLEAR-1 radiosonde data were almost entirely limited to the tropospheric altitudes). Over the S_{raw}'s of interest, the regression almost overlays the one in Figure 2 and this explains why the results were "robust" to model change.

Table 5. Isoplanatic Angle Figures of Merit From Alternative Model "Z^{5/3}"

Flight Number	AFGL	Radiosonde Models "Z ^{5/3} " x 10 ⁷		Thermosonde "Z ^{5/3} " x 10 ⁷ (Experiment)**
		HUF**	VZ**	
1	3.45*	1.84	3.35	4.50
2	6.92*	1.30	3.52	10.9
3	5.00	1.49	3.40*	3.81
4	4.91	3.36*	13.0	2.67
5	6.48	2.80*	5.92	3.76
7	3.97	0.618	2.39*	2.42
8	5.24	1.25	2.42*	2.45
9	3.99*	0.665	2.72	5.05
10	6.31	0.860	3.83*	4.79
11	6.79	4.93*	5.42	2.03
TOTAL	3	3	4	

* = closest model

** exactly as in Table 2

MODEL: 1.566 + 29.62 S_{raw}. Troposphere

0.5084 + 37.01 S_{raw}. Stratosphere

Table 6. Scintillation Variance Figures of Merit From Alternative Model "Z^{5/6}"

Flight Number	AFGL	Radiosonde Models "Z ^{5/6} " x 10 ¹⁰		Thermosonde "Z ^{5/6} " x 10 ¹⁰ (Experiment)
		HUF**	VZ**	
1	1.55	0.857	1.71*	1.78
2	3.51*	0.595	1.73	4.10
3	2.74	0.688	1.84*	1.73
4	2.00	1.48*	5.63	1.14
5	2.50	1.25*	2.82	1.57
7	1.40	0.252	0.982*	0.918
8	2.15	1.575	1.20*	0.986
9	1.85*	0.348	1.33	2.36
10	2.97*	0.432	1.85	2.35
11	2.73	2.21*	2.75	0.773
TOTAL	3	3	4	

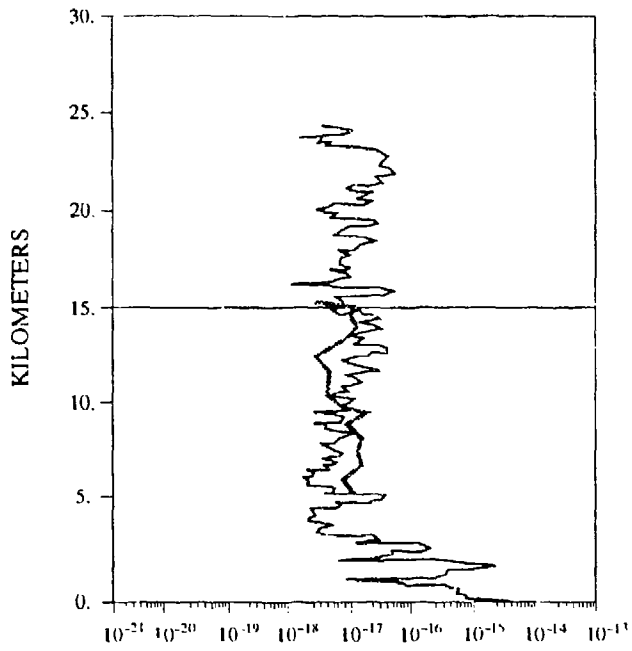
* = closest model

** exactly as in Table 3

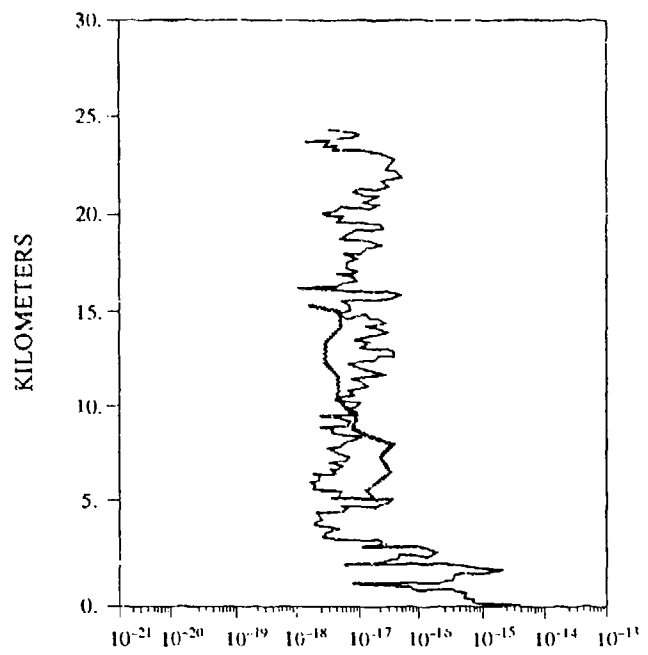
MODEL: 1.566 + 29.62 S_{raw}. Troposphere

0.5084 + 37.01 S_{raw}. Stratosphere

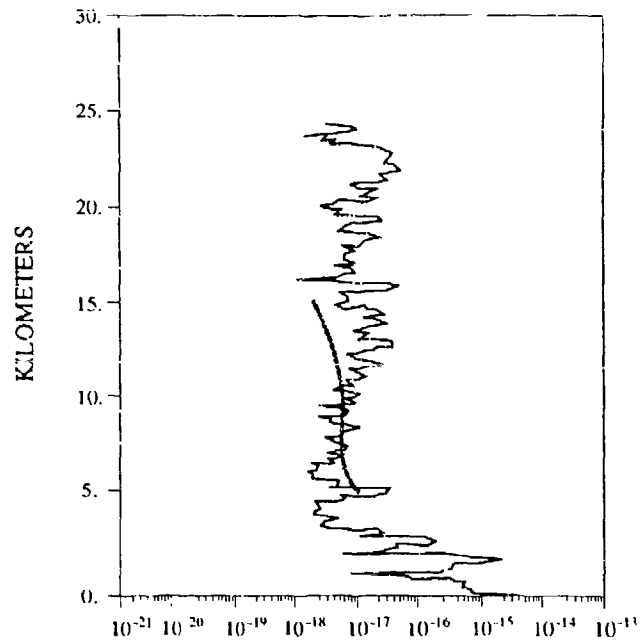
NOTE: In Tables 5 and 6, flight number 6 was omitted.



AFGL ESTIMATE C_n^{**2}

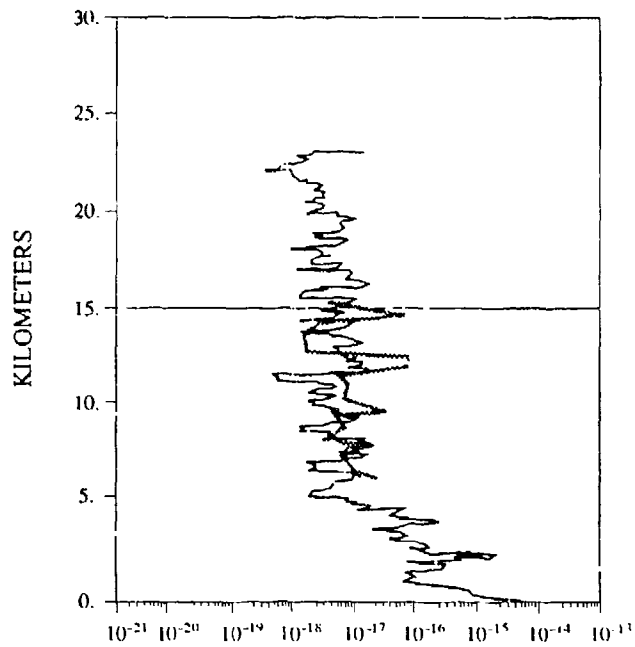


VAN ZANDT ESTIMATE C_n^{**2}

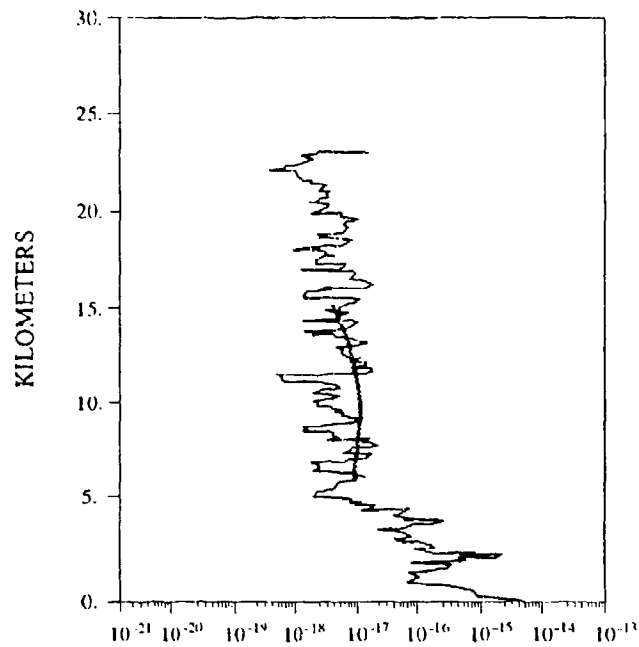


HUFNAGEL ESTIMATE C_n^{**2}

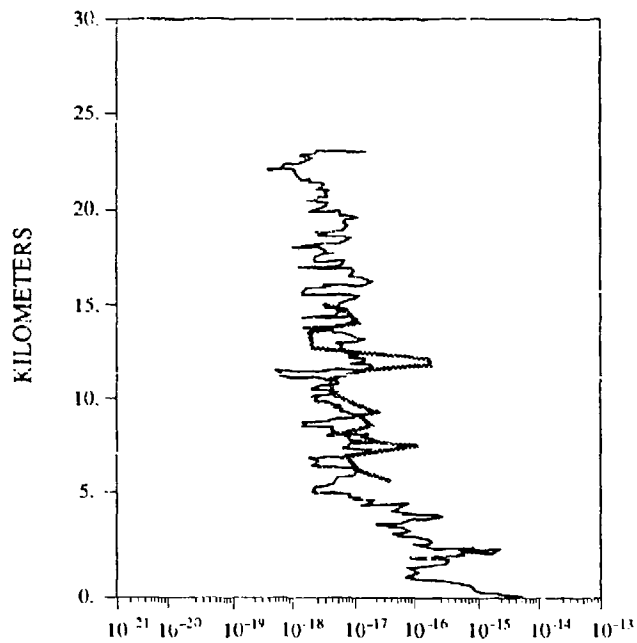
Figure 4 — #1 Tables 1, 2, and 3. (Model and Data Comparisons in CLEAR-1).



AFGL ESTIMATE C_N^{**2}

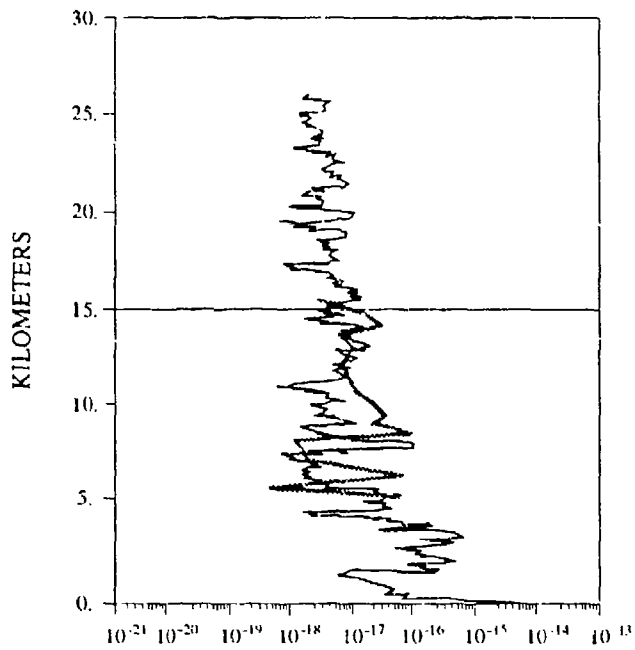


HUFNAGEL ESTIMATE C_N^{**2}

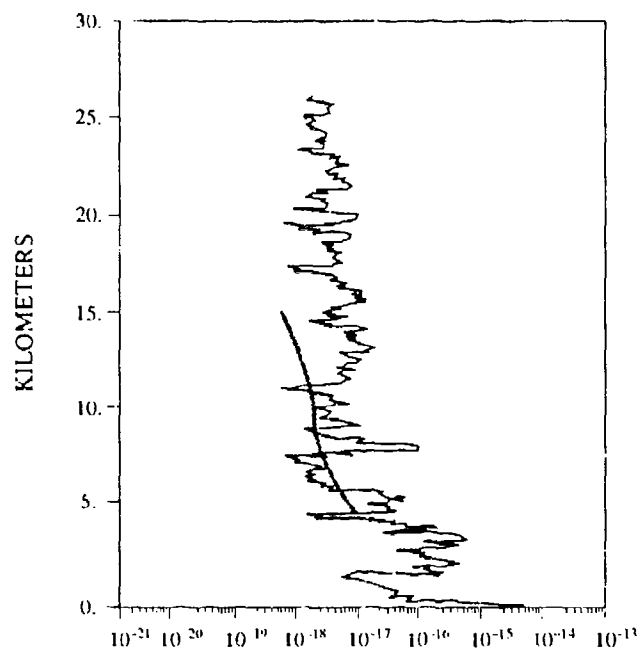


VAN ZANDT ESTIMATE C_N^{**2}

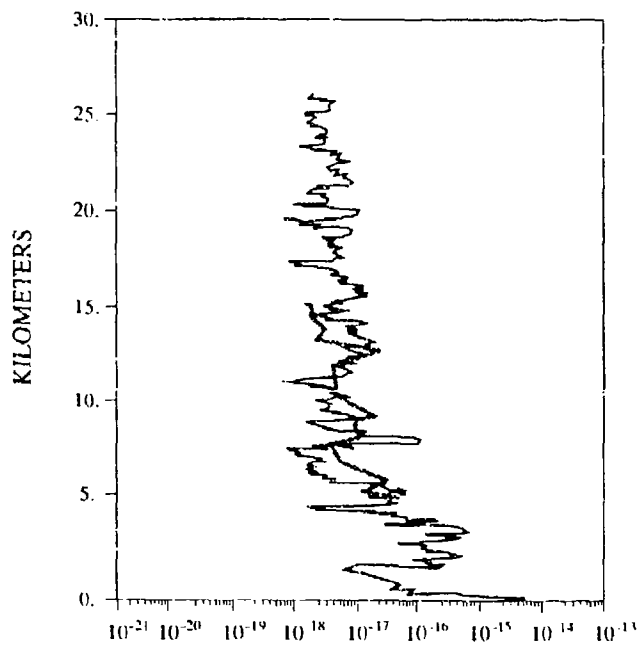
Figure 5 — #4 in Tables 1, 2, and 3. (Model and Data Comparisons in CLEAR-1).



AFGL ESTIMATE C_n^{**2}



HUFNAGEL ESTIMATE C_n^{**2}



VAN ZANDT ESTIMATE C_n^{**2}

Figure 6 — #10 in Tables 1, 2, and 3. (Model and Data Comparisons in CLEAR-1).

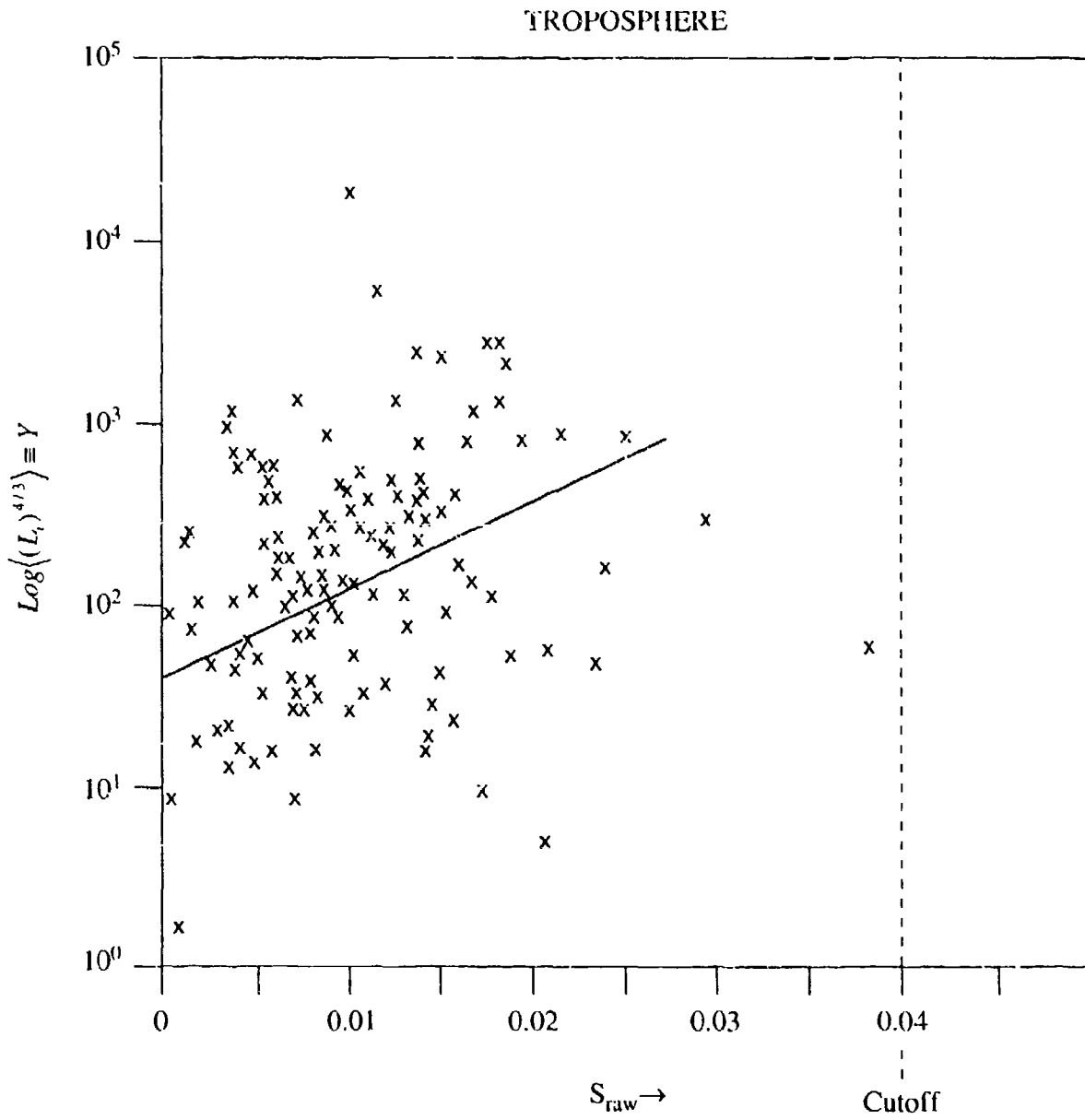


Figure 7 — Tropospheric Alternative Model.

5. Comparisons, Hawaiian Program 1984 Data

In 1984 we conducted a field program in Hawaii during which a number of instrument packages containing P and T sensors were launched and for which a tracking system gave velocities. These data differed in several ways from standard radiosonde data but they nevertheless provided useful information. They gave, for example, an opportunity to perform stratospheric comparisons (an opportunity not given in CLEAR-1). Secondly, the P and T measurements were provided at a relatively high resolution (around 20 m) in comparison to radiosondes (300 m and larger). In this way we could better ascertain correlations between model and *in situ* measurements of C_n^2 .

Again we employed the model given in Eq. (9); but this time the P and T data were pre-processed. Figure 8 shows an example of raw P, T, and velocity data. The velocity resolution (unlike P and T) was very much like that found in standard radiosondes. For this reason the velocity data were not pre-processed.

To smooth P and T (and report out M^2 at equally spaced altitudes of 300 m) we fitted an 18 point parabola around the altitude of interest (that is, at each extreme of the 300 m interval for T). The results were reported at the midpoints of these intervals for $\Delta T/\Delta z$ and then T and P were calculated (in the same manner) at those same midpoints. Then the shears were calculated from the raw velocities and the model [Eq. (10)] was applied as was described in Section 3. Figures 9 and 10 give the two cases that extended into the stratosphere (the others did not). The correlations were encouraging. Tables 7 and 8 are based on the figure of merit. In this case the AFGL model performed better than the other models, but raw radiosonde data represents the type of data it must use in our application. Nevertheless these results argue for more research to be done, in view of the success of the AFGL model.

One detail regarding Table 7 should be mentioned. When it was constructed (1985) we did not place the lower limit of the integral at 5 km but at the altitude where data commenced.

Minimum Z = 2.969768 Maximum Z = 26.595832
Minimum Temp = 192.393163 Maximum Temp = 283.645674

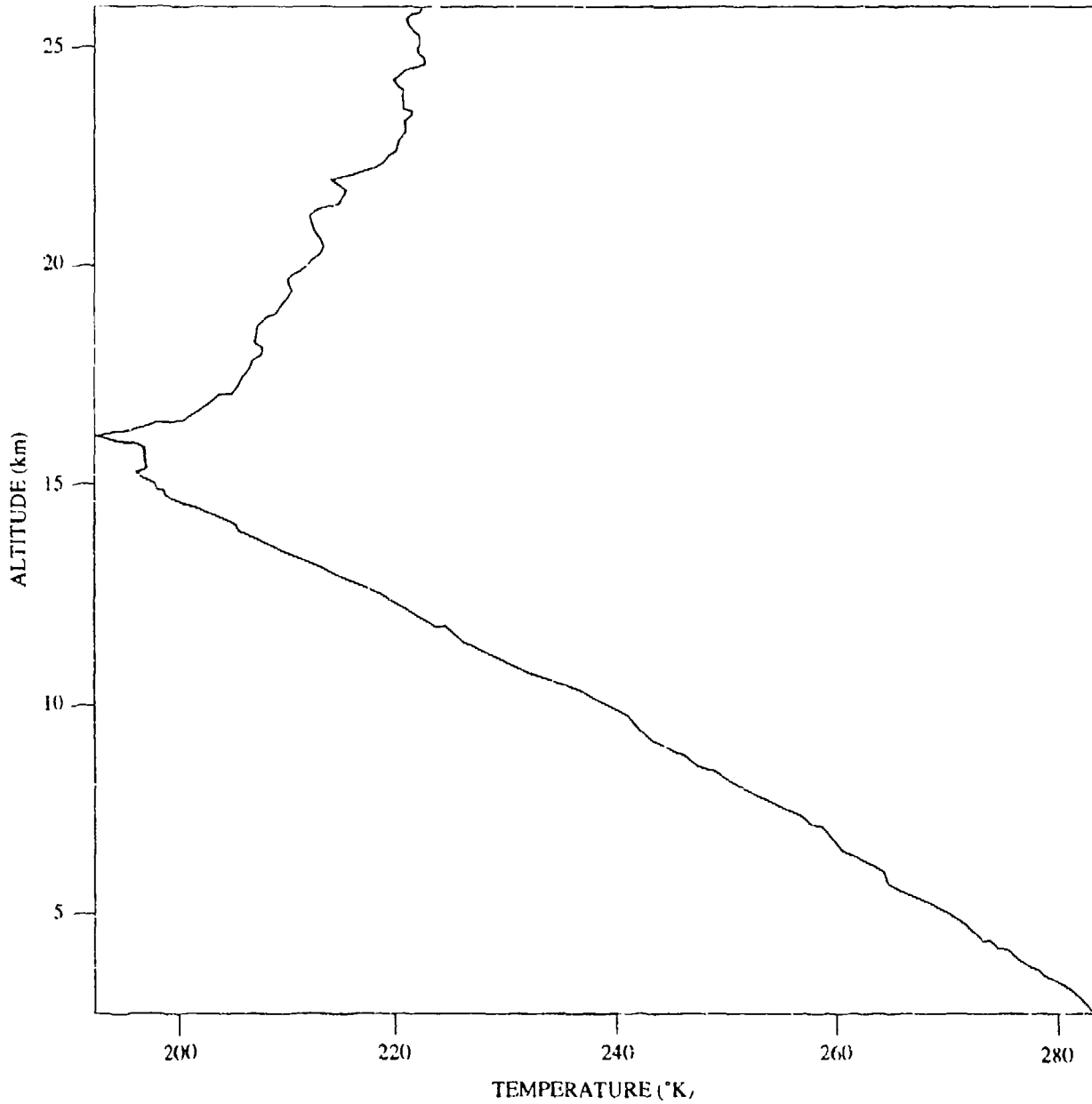


Figure 8-A — Radiosonde Temperature Measurements (Hawaii, 1981 #05) °K.

Minimum Z = 2.969768
Minimum Speed = 4.115556

Maximum Z = 26.595832
Maximum Speed = 28.294444

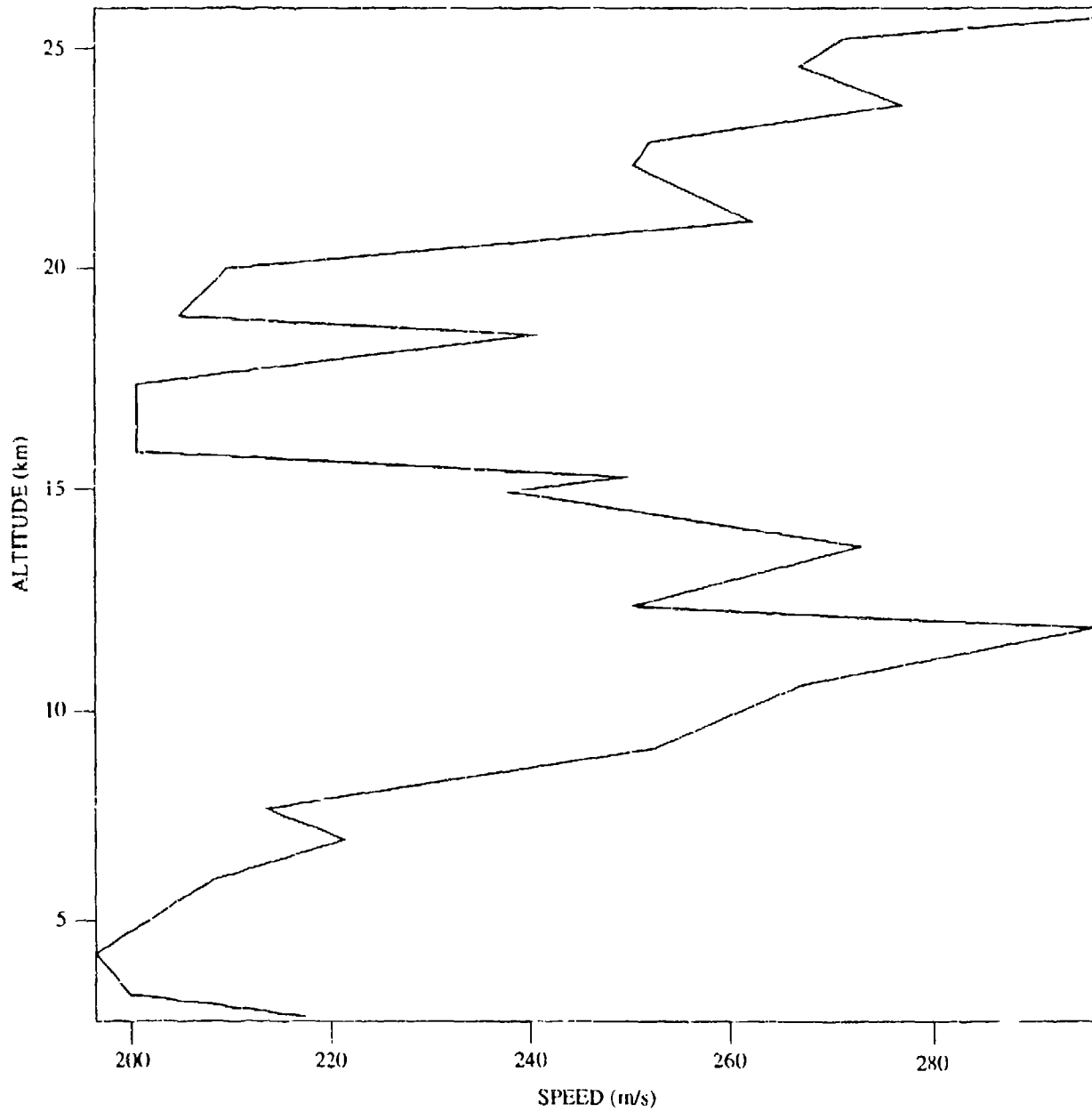


Figure 8-B — Radiosonde Wind Speed Measurements (Hawaii, 1984 #05) m/s.

Minimum Z = 2.969768

Maximum Z = 26.595832

Minimum V E-W = 26.588081

Maximum V E-W = 27.357959

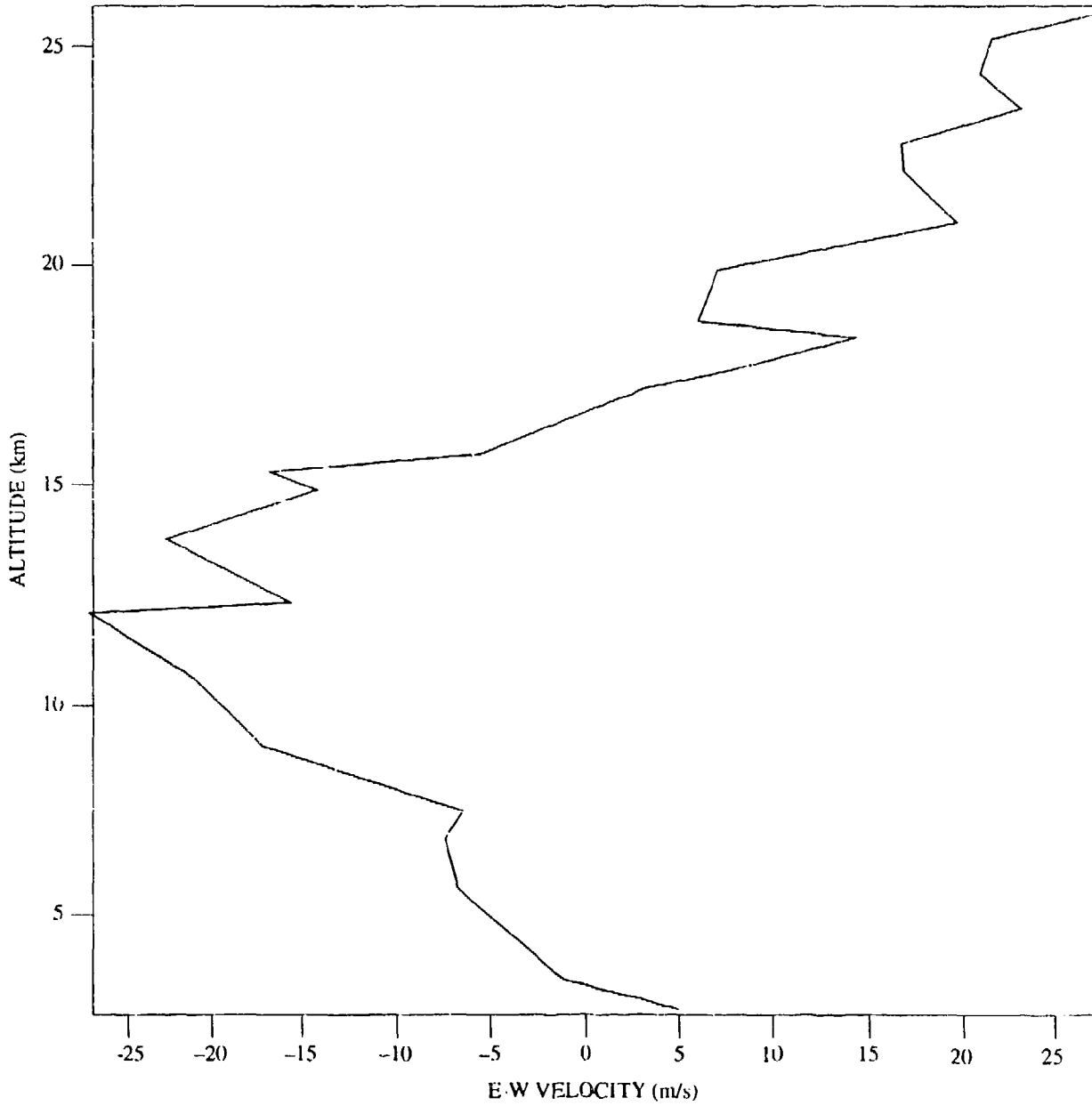


Figure 8-C — E/W Wind Velocity (Hawaii, 1984 #05) m/s.

Minimum Z = 2.969768
Minimum V N-S = 9.677270

Maximum Z = 26.595832
Maximum V N-S = 4.823946

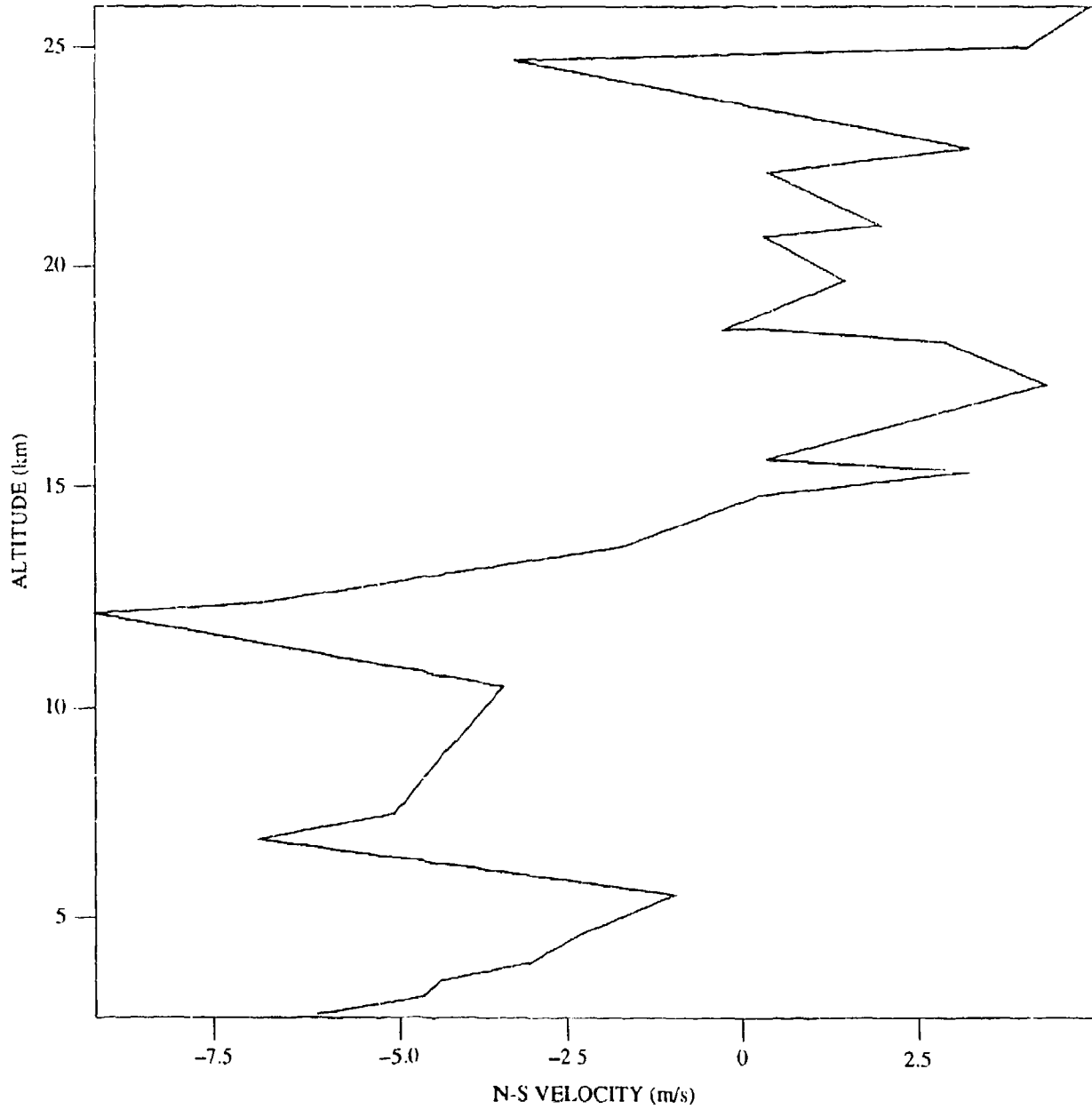


Figure 8-D — N/S Wind Velocity (Hawaii, 1984 #05) m/s.

Minimum Z = 2.969768
Minimum Press = 20.768661

Maximum Z = 26.595832
Maximum Press = 706.637421

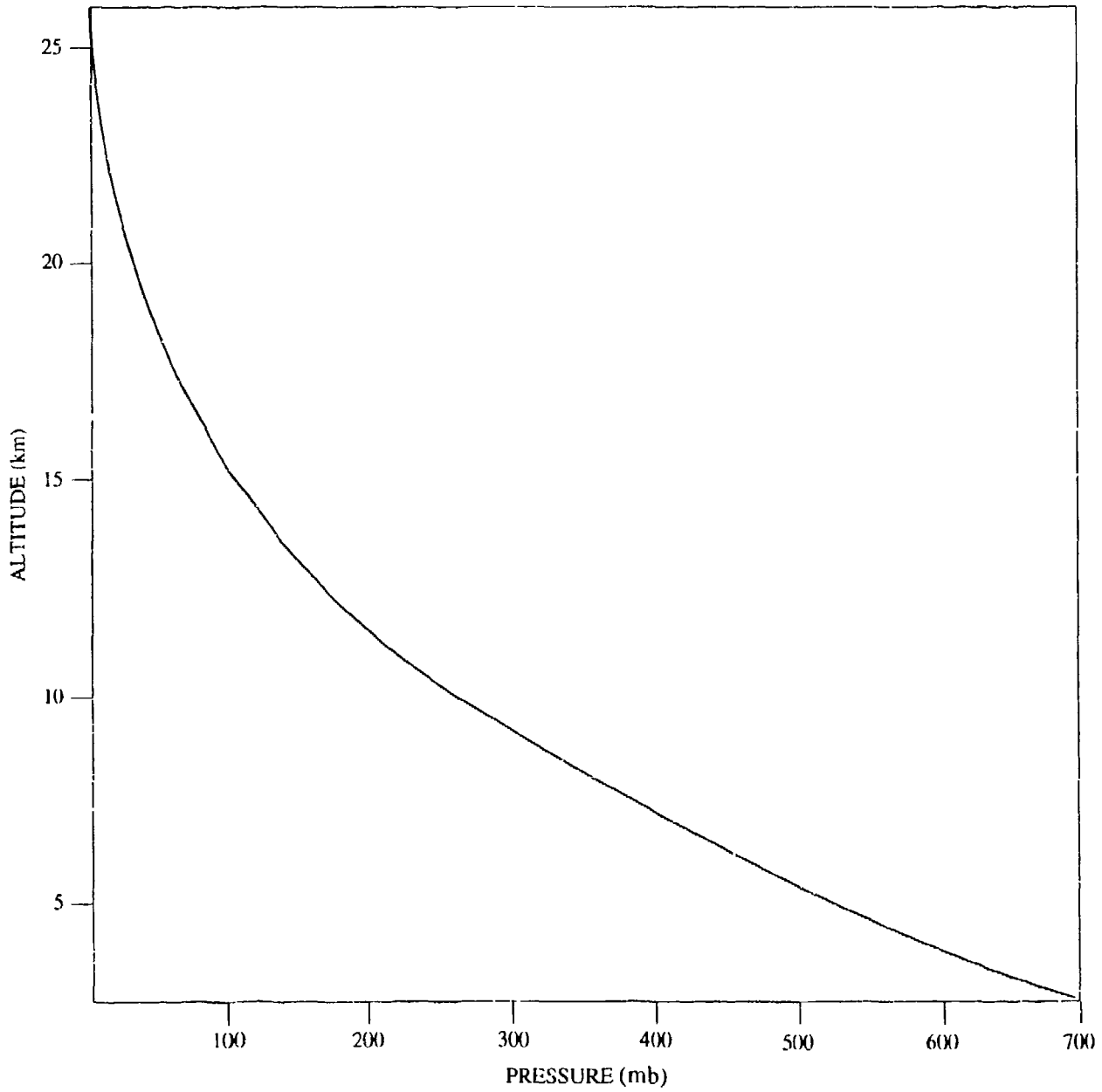


Figure 8-E -- Pressure (Hawaii, 1984 #05) mb.

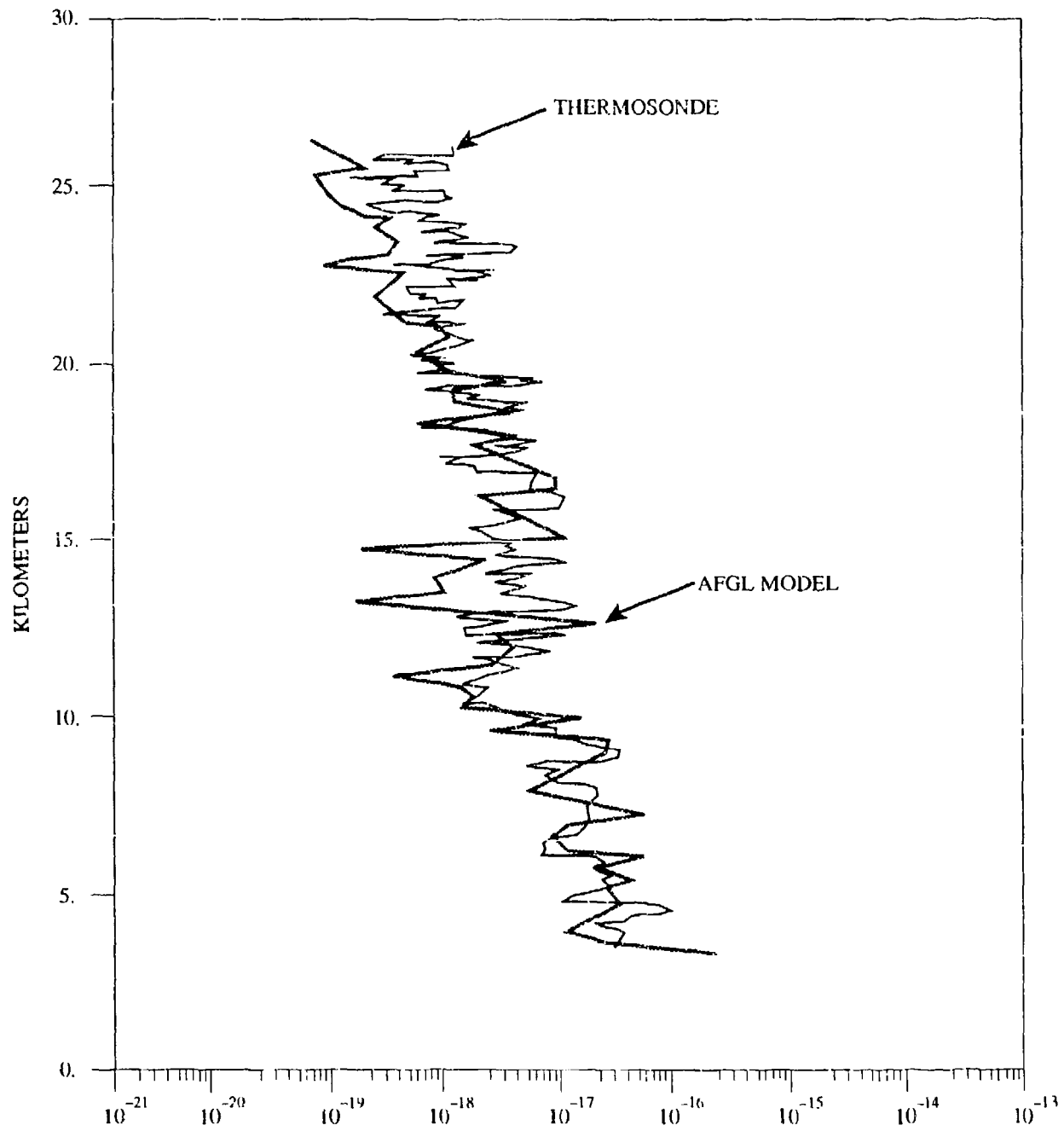


Figure 9-A — Models and Data Comparisons HAW 01 (1984).

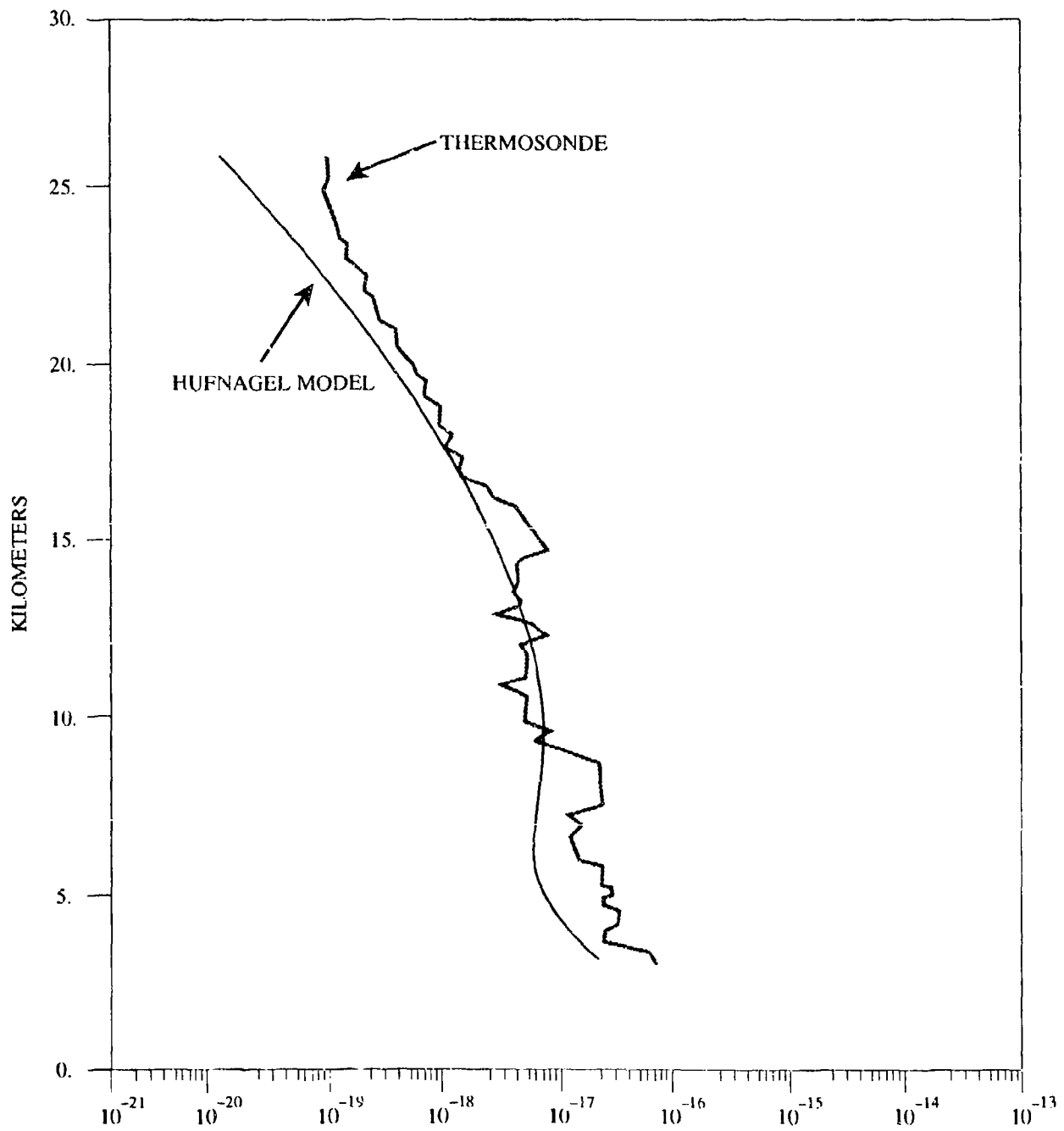


Figure 9-B — Models and Data Comparisons HAW 01 (1984).

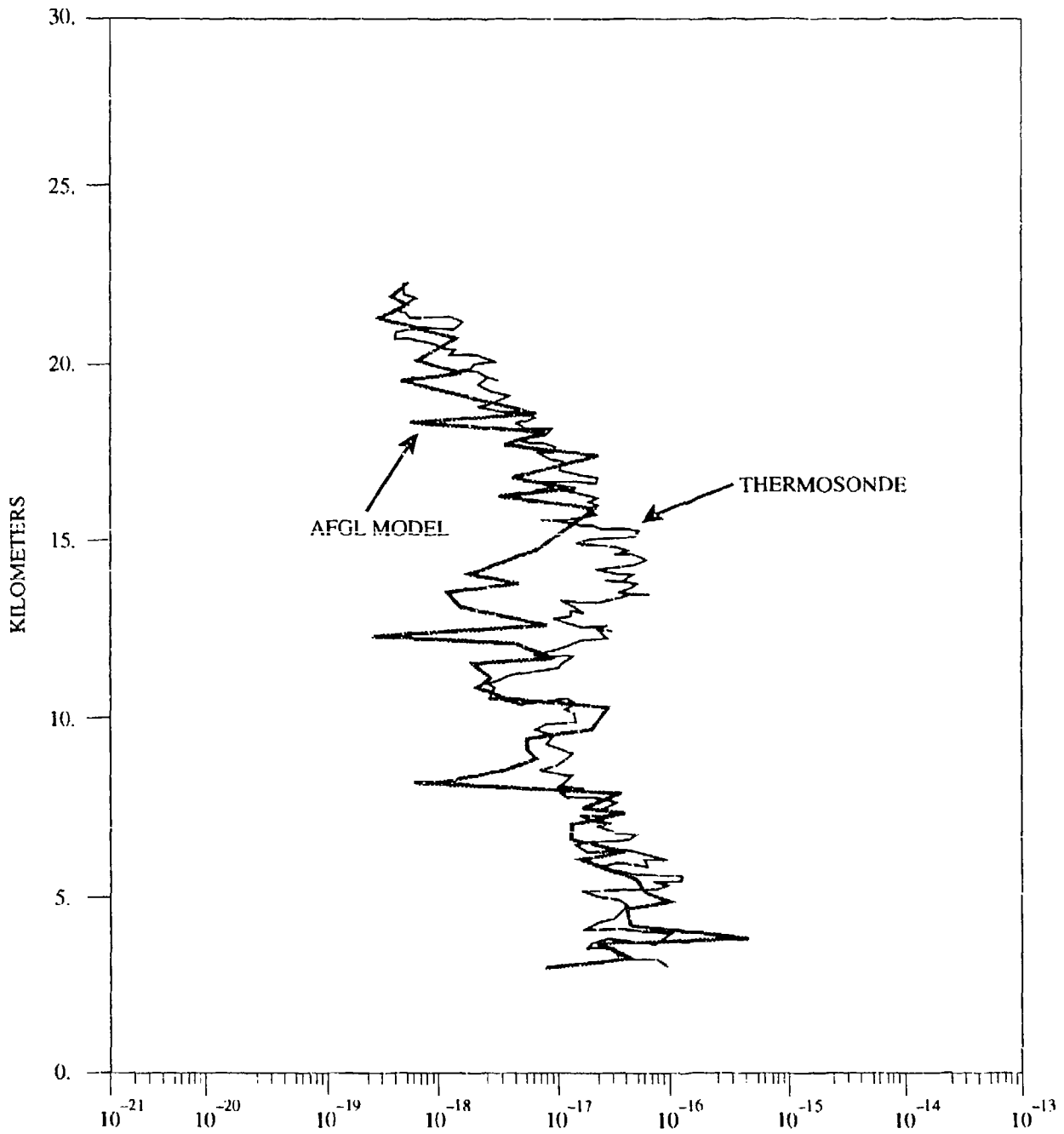


Figure 10-A — Models and Data Comparisons HAW 49 (1984).

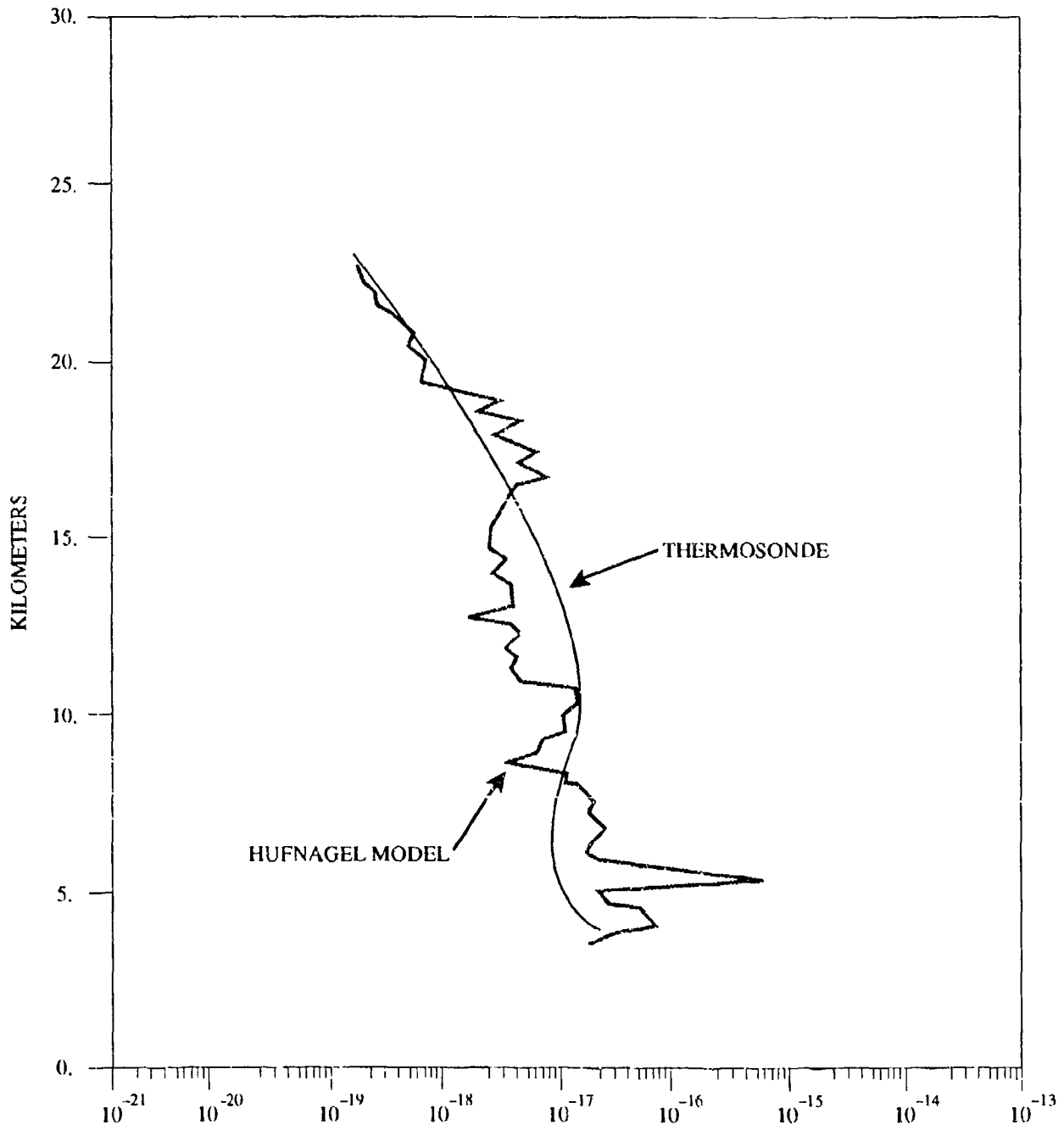


Figure 10-B — Models and Data Comparisons HAW 49 (1984).

Table 7. Isoplanatic Angle Figures of Merit for the 1984 Hawaiian Program Data
 $[(Z^{5/3})^{-3/5} \times 10^{-3}]$

RUN	AFGL	Thermosonde		(Experiment)
		HUF**	VZ**	
1	6.72*	8.91	8.89	7.77
22	11.6*	37.3	16.0	11.8
37	3.33*	5.66	1.88	3.53
38	6.80*	10.2	4.48	6.20
45	7.86	14.5*	4.08	12.4
49	5.69*	6.42	7.51	4.00

TABLE 8. Scintillation Variance Figures of Merit for the 1984 Hawaiian Program Data
 $[(Z^{5/6}) \times 10^{10}]$

RUN	AFGL	Thermosonde		(Experiment)
		HUF**	VZ**	
1	2.41	1.47*	1.62	1.56
22	1.56*	0.258	0.877	1.56
37	6.15*	3.11	12.8	6.19
38	2.43*	1.28	4.36	2.28
45	2.62*	0.861	6.95	1.33
49	3.24*	2.47	2.83	4.93

6. Comments, and Suggestions for Future Work

If one assumes, as we have, that the only useful application of radiosonde type models is in connection with standardized radiosonde data, then it follows that future research should use such standardized data exclusively. It may be objected that high resolution data obtained from the thermosonde balloon package are preferable because of the advantage of collocation; and, furthermore, one could smooth this data to a resolution of 300 m to simulate radiosonde data. Our experience directly contradicts this and we therefore strongly recommend against further work with non-standard radiosonde data. Further arguments can be supplied; but, a model should be designed for the data intended.

One possible extension of the AFGL model that we did not test was a model based upon a variable S_c value. This may be worth pursuing in the future. At this point we would like to mention some of the attempts that did not seem to be beneficial in this project. This will help others who might want to continue the work to avoid the same pitfalls. At one point we designed a model with a variable resolution. (for example, 300 m, 600 m, 1 km, etc.) and let the actual resolution pick the Y regression to be used. These variable models consistently performed less effectively than our fixed 300 m model. Perhaps our high resolution velocity data base was too small and perhaps a future effort along these lines should be based on such scaling laws as are found in the work of Essenwanger.¹⁰ Another unfruitful avenue was the attempt to improve the Y-regression by using a parabola instead of a straight line. This led to bad results and should therefore be avoided.

The last blind alley we will mention is our attempts to use linear prediction techniques in place of the statistical shear model for Y. We had hoped to produce a linear predictor to interpolate shears in the low resolution radiosonde velocity measurements. This linear predictor was based upon the high resolution data. It failed for reasons unknown to us at the time. We now know that the explanation lies in the physical basis of linear predictors. The latter is described in Dewan¹¹ (1985) and in essence it is that a linear predictor represents a dynamical system (or a filter) stimulated by random noise, and the predictions consist of this system's behavior after the input noise has ceased. Such a system will output fluctuating signals after the noise input is terminated but eventually they die out. Unfortunately, the linear predictor for velocity fluctuations is highly damped, so highly damped that the fluctuations die out almost instantly. For this reason they were useless for interpolating high resolution (10 m) shears between 300 m velocity points.

One final point should be made. It is that we still do not possess a reasonably large number of stratospheric and tropospheric comparisons between the models based on radiosondes under very different conditions. For example, under low wind conditions the Hufnagel model performs very badly. Clearly the next step would be to remedy this situation.

It should be noted that we learned during the course of this research that solar heating of the thermosonde probes during the daytime could cause their measurements to be in error. Only night measurements can be trusted at this time. (See Reference 12.)

7. Conclusions

The AFGL model is much simpler than the VanZandt model. With the data available to us, it was not possible to establish which of the two superior models (compared to the Hufnagel model) was actually the best on the basis of performance. In CLEAR-1, the NOAA (VanZandt and Warnock) model was rated best; when the Hawaiian campaign data were used, the AFGL model performed best. If future tests show that the models remain more or less comparable in performance, then the decision of which one to use could be made on the basis of simplicity; the AFGL model would then be chosen.

References

1. Tatarski, V.I. (1961) *Wave Propagation in a Turbulent Medium*, McGraw-Hill, N.Y.
2. Dewan, E.M. (1980) *Optical Turbulence Forecasting: A Tutorial* AFGL-TR-80-0030, NTIS:ADA 086 863.
3. Hufnagel, R.E. (1978), Propagation Through Atmospheric Turbulence, Ch 6 in *The Infrared Handbook*, Wolfe, W. L. and Zissis, G. J. editors.
4. Van Zandt, T.E., Gage, K.S. and Warnock, J.M. (1981) An Improved Model for the Calculation of Profiles of C^2_n and ϵ in the Free Atmosphere From Background Profiles of Wind, Temperature and Humidity, 20th Conference on Radar Meteorology, Nov 1981, American Meteorological Society, Boston, MA.
5. Pond, S.R.W. Steward and R.W. Burling, (1963) Turbulence Spectra in the Wind over Waves, *J. Atm. Sci.*, 20:319 - 324.
6. Tennekes, H. and Lumley, J.L. (1972) *A First Course in Turbulence*, MIT Press, Cambridge, MA. 1972.
7. Dewan, E.M. and Good, R.E. (1986) Saturation and the 'Universal' Spectrum for Vertical Profiles of Horizontal Scalar Winds in the Atmosphere, *J. Geophys. Res.*, 91:2742 2748.
8. Dewan, E.M., Grossbard, N., Quesada, A. and Good, R.E. (1984) Spectral analysis of 10 m Resolution Scalar Velocity profiles in the Stratosphere, *Geophys. Res. Lett.* 11:80-83, [correction, p. 624].
9. Bevington P.R. (1969) *Data Reduction*, McGraw-Hill.
10. Essenwanger, and Billions, N. (1965) *On Wind Distributions for Smaller Shear Intervals*, Report No. RR-TR-65-4, NTIS No. AD 466161.
11. Dewan E.M. (1985) *A Review of Maximum Entropy Spectral Analysis and Applications to Fourier Spectroscopy*, AFGL-TR-85-0091, ADA 164698.
12. Brown, J., E. Dewan, E. Murphy, P. Thomas (1978) *Study of Possible Solar Heating Effects on Thermosonde Probes—Error Analysis*, GL-TR-89-0178, ERP No. 1034, ADA-218-116 (NTIS).

Appendix A

This appendix contains the entire report presented in 1986 at a conference (compare with Good et al. 1988).^{A1} It includes a description of the Van Zandt and Hufnagel models. It also provides additional model comparisons. Perhaps one more asset is that it will provide an alternative description to compare with the main text.

MODELING C_N^2 PROFILES FROM RADIOSONDE DATA

E. M. Dewan, R. E. Good, R. Beland, J. Brown
Hanscom AFB, Bedford, MA 01731-5000

ABSTRACT

The structure constant for the fluctuations of the optical index of refraction, C_N^2 , is the key to the design of adaptive optical systems so that the effects of turbulence on laser beam propagation can be minimized. This paper compares three models which convert standard radiosonde data into C_N^2 profiles. Models are compared to directly measured values of C_N^2 obtained by balloon borne thermosondes.

A1. INTRODUCTION

The purpose of this section is to compare the performance of the three existing models for converting radiosonde data into C_N^2 vertical profiles. The outputs of these three models will be compared to actual *in situ* experimental thermosonde measurements. In addition to direct profile comparison a parametric comparison will be made based on isoplanatic angle calculations.

During CLEAR 3 we obtained three thermosonde and four radiosonde profiles on two simultaneous dates and they were all launched from WSMR. They were not launched on the same hours nor from the same locations however. Figure A1 shows a comparison of a radiosonde temperature profile taken at one location and a thermosonde flight temperature profile taken on the same day but from a different location. As can be seen, these profiles are quite similar, and the main differences could perhaps be attributed to differences in resolution.

In order to eliminate effects of boundary layer turbulence (which are outside of these model capabilities) we intentionally ignored all information below 5 km. This has the added benefit of eliminating the need to include humidity effects which, strictly speaking, do not extend beyond about 7 km.

Our conclusion will be that the results suggest that the AFGM model may be superior in performance and simplicity to the Van Zandt model. More data would be needed however to confirm that this is true in general. Also, as was expected, the Hufnagel model fails under the experimental conditions of CLEAR 3.

A2. C_N^2 Profile Models

Historically, the oldest and simplest of these models is the one due to Hufnagel (Reference A1). It is given by

$$C_N^2(z) = [8.2 \times 10^{-56} V^2 Z^{10}] e^{-(z/10^4)^{10}} + (2.7 \times 10^{-16} e^{-(z/15000)}) \quad (1)$$

where Z is the altitude in meters, V^2 is the spatial average of the wind speed squared over the altitude regions on 5km to 20km, and C_N^2 is given in units of $m^{-2/3}$. The simplicity of this model resides in the fact that only V^2 , a single parameter, is required of the radiosonde data.

The second model is due to Van Zandt et al, (References A3, A4). It is the most complex of three under discussion. In order to assign a value of C_N^2 to a specific height region one needs a number of parameters from the radiosonde data. These are temperature, T , in °K, pressure P in mb, temperature gradient, dT/dz , specific humidity, q , and its gradient dq/dz , and the vector wind shear from the velocity measurements, S . Since this model is based in part upon the Richardson number (Ri) criterion, which is given by $Ri \equiv N^2/S^2 < 1/4$, where N is the buoyancy frequency, the two key parameters are given by N^2 and S^2 . That is to say N^2 and S^2 must be fed into the model on the basis of the data. As has been mentioned already, we will omit the use of q and dq/dz in this report (q is specific humidity).

A second and crucial piece of this model is given by the relation

$$C_N^2 = 2.8 M^2 L^{2/3} \quad (2)$$

(See Tatarski, Reference A5) where L is the "outer length". In the present context this is taken to mean a representative scale associated with turbulent layer thickness. The parameter M , which is the factor giving the gradient of the index of refraction, and hence the bridge between L and C_N^2 , is given by

$$M = \frac{-79 \times 10^{-6} P N^2}{g \cdot T} \quad (3)$$

where P is in mb and T in °K, N is s^{-1} and g is the acceleration of gravity. The definition of N is given by

$$N^2 \equiv \frac{g \left(\frac{dT}{dz} + \gamma \right)}{T} \quad (4)$$

where γ is the dry adiabatic lapse rate of 9.8×10^{-3} ($^{\circ}\text{K}/\text{m}$). In the above equations suitably averaged quantities are assumed.

In the development of this model, Van Zandt et al. assume that shears and temperature gradients on a very small scale (relative to the scale of radiosonde data) are the cause of the turbulent layers. This smaller scale they refer to as the microscale. They make a number of assumptions regarding the probability distribution of microscale windshears and temperature gradients. For example they assume a Rice-Nakagami distribution for the absolute values of vector wind shears and a Gaussian distribution for the temperature gradients affecting N^2 . They also assume that the joint probability distribution for L , S^2 , N^2 , and dq/dz can be factored. They also made use of the statistical findings of Essenwanger, Rosenberg and Dewan, Cadet, and Adelfang (see References A3 and A4 for the references). Finally their model is predicated on the assumption that the turbulence under consideration is caused by gravity waves. Reference 3 should be consulted for all the details as well as for a very well documented computer program for this model. As can be seen, it is apparently somewhat complex. The key equation for the Van Zandt model is

$$C_N^2(z) = \int_0^{\infty} dL \int_{R_1 < L} dS dN P^i(L, S, N) C_n^2(L, N) \quad (5a)$$

The third model we shall call the "AFGL model." It is the most recent one to date and it is simpler than the above case despite the fact that the physics behind it is essentially the same in the sense that both R_1 and Eq. (2) enter into its construction. Its implementation relies on the simple relation

$$C_N^2 = 2.8 [R_1(z)]^2 (0.1)^{4/3} 10^{Y(z)} \quad (5b)$$

As before, P and T from the radiosonde determine M^2 from (3) and (4), and Eq (2) leads to (5). The factors $(10^Y(0.1)^{4/3})$ determine $L^{4/3}$ in a statistical manner to be described. The factor (0.1) arises from a rule of thumb that the outer length, L is of the order of one tenth the thickness of a turbulent layer. In the implementation, Y is obtained from

$$Y = C_1 + C_2 S \quad (6)$$

where S is the "raw shear" (not the microscale shear) directly measured from the radiosonde data. The term Y arises from the definition $\log \mathcal{L}^{4/3} \equiv Y$, and 10^Y determines the most probable median value of $L^{4/3}$ in the altitude region under consideration. Again, following the lead of the Van Zandt approach this model assumes that micros shears cause turbulence; however, the value of N^2 used in the Richardson number criterion is no longer data dependent in the AFGL model. Instead, the value of N^2 is based on a model atmosphere during the creation of the model. In the application of the model the temperature data is used to calculate M in Eq. (5) as already mentioned. Note that this is a departure from the Van Zandt model in that *microscale* temperature gradients are not in the theoretical picture. On the other hand, the AFGL model does incorporate radiosonde measurements of temperature in the M^2 factor.

Since the value of N^2 used in the Richardson number criterion is not data dependent, the AFGL model is actually composed of two models, one for the stratosphere and one for the troposphere. During application, the results from these two models are simply joined by a straight line across the tropopause. These two models consist of:

$$\begin{aligned} Y &= 1.566 + 29.62 S & \text{TROPOSPHERE} \\ Y &= 0.508 + 37.01 S & \text{STRATOSPHERE} \end{aligned} \quad (7)$$

Unlike the Van Zandt model, the AFGL model has not been explained in detail anywhere in print and hence it may be useful to describe how we arrived at Eq. (7). We were fortunate to be in possession of a unique set of very high resolution wind profiles (10 m). These we believe represent actual measurements of the microscale motions and hence we, in a sense, had direct access to the data relevant to the microscale turbulent layers. On the basis of the previously mentioned standard atmospheric value of N^2 we arrived at 0.0155 s^{-1} and 0.030 s^{-1} * for the tropospheric and stratospheric values of the critical microshear (that is, the shear necessary to cause turbulence on the basis of the Richardson criterion). In this way we could assign layer thicknesses to the microscale data. In other words, a thickness \mathcal{L} was assigned to each region where the microshears exceeded the critical value.

Since the resolution of the radiosondes is of the order of 300m, we related the "raw shears," that is the shears across 300m of the microscale winds, to the value of $\log \overline{\mathcal{L}^{4/3}}$ where the over bar represents the weighted average. Thus we used

$$10^r \equiv \sum_i \mathcal{L}_i^{4/3} \frac{(\mathcal{L}_i)}{(300m)} \quad (8)$$

for each segment. On the basis of linear regression we obtained Eq. (7).

In summary, the AFGL model is applied to radiosonde data by inserting the measured values of T, P, and V (the vector velocity) and/or the appropriate derivative etc. into (7) and (5b) using (4) and (3). The results from (5b) are then plotted as a function of height. This model seems to be simpler in concept and application than the Van Zandt model. We now turn to the comparison of results.

* USA Standard ATM actually gives data implying $.025 \text{ s}^{-1}$ for the troposphere and 0.045 s^{-1} for the stratosphere in previous work. The above values were chosen because they gave better performance in previous comparisons.

A3. Model Profile Comparison

Figure A2 shows a representative comparison between the model C_N^2 profile and the *in situ* measurements. The most obvious feature of this comparison is the fact that the Hufnagel model profile is far too low in C_N^2 values as compared to the data. In this respect it has failed to give adequate results. There is reason not to be surprised by this situation; namely, it is well known that the Hufnagel model will do this under conditions where the winds are relatively weak such as was the case for CLEAR 3.

Another salient feature is the fact that both the Van Zandt and AFGL models give lower C_N^2 values than the data in the stratosphere. One possible interpretation is that these models both perform less adequately in the stratosphere. The same holds for the Hufnagel model. Another interpretation (in the context of possible solar heating effects on the thermosonde probe)* is that in actual fact the data are overly large due to the heating, in other words it is possible that the data and not the models are not to blame. Parenthetically it should be mentioned that Van Zandt's (et al.) model used here is based on Reference A3 not Reference A4.

Our parametric characterization is based on the well known and important isoplanatic angle θ_o . It is related to the C_N^2 profile through the relation

$$\theta_o (\text{rad}) = \left[2.95 \left(\frac{2\pi}{\lambda} \right)^2 I \right]^{-3/5} \quad (9)$$

where

$$I \equiv \int_{5 \times 10^3 \text{ m}}^{z_{\text{max}}} C_N^2(z) (z - z_g)^{5/3} dz \quad (10)$$

and where meters are used throughout, z_g is the altitude of the ground station (zero here in the comparison role), and λ is the wavelength of the optical signal. Note the lower limit on the integral. In practice it would start at z_g but our purpose is not to calculate the true θ_o but rather to compare models and ignore the boundary layer as has been already explained.

Table A1 lists flight dates and times as well as values of z_{max} for overlap. The comparison parameter I shows that the AFGL model gave the closest agreement with the data. Table A2 gives a similar comparison in term of θ_o and Table A3 gives the "percentage" comparisons. If the thermosonde data are assumed to be the final arbiter of this comparison, then the AFGL model was the best one. On the other hand, unanswered questions remain as have been pointed out in the text. Furthermore we need more comparisons under varied conditions before the issue can be settled. Our modest conclusion is that if the AFGL model were merely to perform as well as the Van Zandt model, it would still be, in a sense, superior because it is a much simpler model.

*This possibility is presently under very active investigation. NOTE added: It turns out, as mentioned in the main text, that *daytime* thermosonde measurements are unreliable. In fact, they are now totally avoided in current research.

Table A-1. Values of 1×10^7 for Various Radiosonde Models and for Thermosonde Measurements in the Altitude Range of 5 km to z max

Radiosonde Models*					Thermosonde*			Z Max Alt In Common (km)
Date	Launch Time MST	1×10^7			1×10^7 EXP.	Launch Time MST	Ser. No.	
		AFGL	Hufnagel	Van Zandt				
1 Aug 1	8.17 am	11.5	0.994	5.64	4.93	1:44 pm	6474	24.98
2 Aug 2	0.03 am	11.8	1.18	4.00	10.1	11:08 am	6483	25.16
3 Aug 2	0.03 am	11.8	1.18	3.98	12.8	3:19	5306	24.00
4 Aug 2	6.00 am	6.54	1.12	4.71	10.1	11:08 am	6483	25.16
5 Aug 2	6.00 am	6.50	1.12	4.69	12.8	3:19 pm	5306	24.00
6 Aug 2	9.5 am	5.54	0.956	3.61	5.50	11:08 am	6483	16.9
7 Aug 2	9.5 am	5.54	0.956	3.61	8.27	3:19 pm	5306	16.9

* 4 Radiosonde profiles — 3 models, compared to 3 Thermosonde profiles.

Table A-2 — Values of θ_0 for Various Radiosonde Models and Thermosonde Measurements

Model θ_0 (μ -rad)			EXP. θ_0 (μ -rad)		
AFGL	Hufnagel	Van Zandt	Thermosonde	Ser. No.	
4.58	19.9	7.02	7.61	6474	1
4.51	17.9	8.62	4.95	6483	2
4.51	17.9	8.65	4.29	5306	3
6.42	18.5	7.82	4.95	6483	4
6.44	18.5	7.84	4.29	5306	5
7.09	20.4	9.17	7.12	6483	6
7.09	20.4	9.17	5.58	5306	7

Dates, times, and altitude ranges are exactly as in Table 1 in sequence.

Table A-3 — Comparison Between AFGL and Van Zandt Models

No.	AFGL Δ %	VAN ZANDT Δ %
1	-39.8	-7.75
2	-8.89	58.8
3	5.13	-102.0
4	29.7	58.0
5	50.1	82.8
6	-0.42	28.8
7	27.06	64.3
AVE ABS. VAL	23 \pm 19	57 \pm 30

$$\Delta \% \equiv \frac{(\text{MODEL } \theta_o - \text{EXPER. } \theta_o) \times 100}{\text{EXPER. } \theta_o}$$

REFERENCES

- A1. R. E. Good, R. R. Beland, E. A. Murphy, J. H. Brown and E. M. Dewan (1988) "Atmospheric Models of Optical Turbulence", in *Modeling of the Atmosphere*, Proceedings of the SPIE 1988 Technical Symposium on Optics, Electro-Optics and Sensors, 4-8 April, 1988, Orlando, FL, Vol 928, 1988.
- A2. Hufnagel, R. E. (1978), Propagation Through Atmospheric Turbulence, Ch 6 in *The Infrared Handbook*, Wolfe, W. L. and Zissis, G. J. editors.
- A3. Van Zandt, T. E., K. S. Gage and J. M. Warnock (1979), An Improved Model for the Calculation of Profiles of C_N^2 and ϵ in the Free Atmosphere from Background Profiles of Wind, Temperature, and Humidity, 20th Conf. on Radar Meteorology, American Meteorological Society, Boston, MA.
- A4. Warnock, J. M., Van Zandt, T. E. (1985), *A Statistical Model to Estimate the Refractivity Turbulence Structure Constant C_N^2 , in the Free Atmosphere*, NOAA Technical, Memo. ERL AL-10.
- A5. Tatarski, V. I. (1961) *Wave Propagation in a Turbulent Medium*, McGraw-Hill.

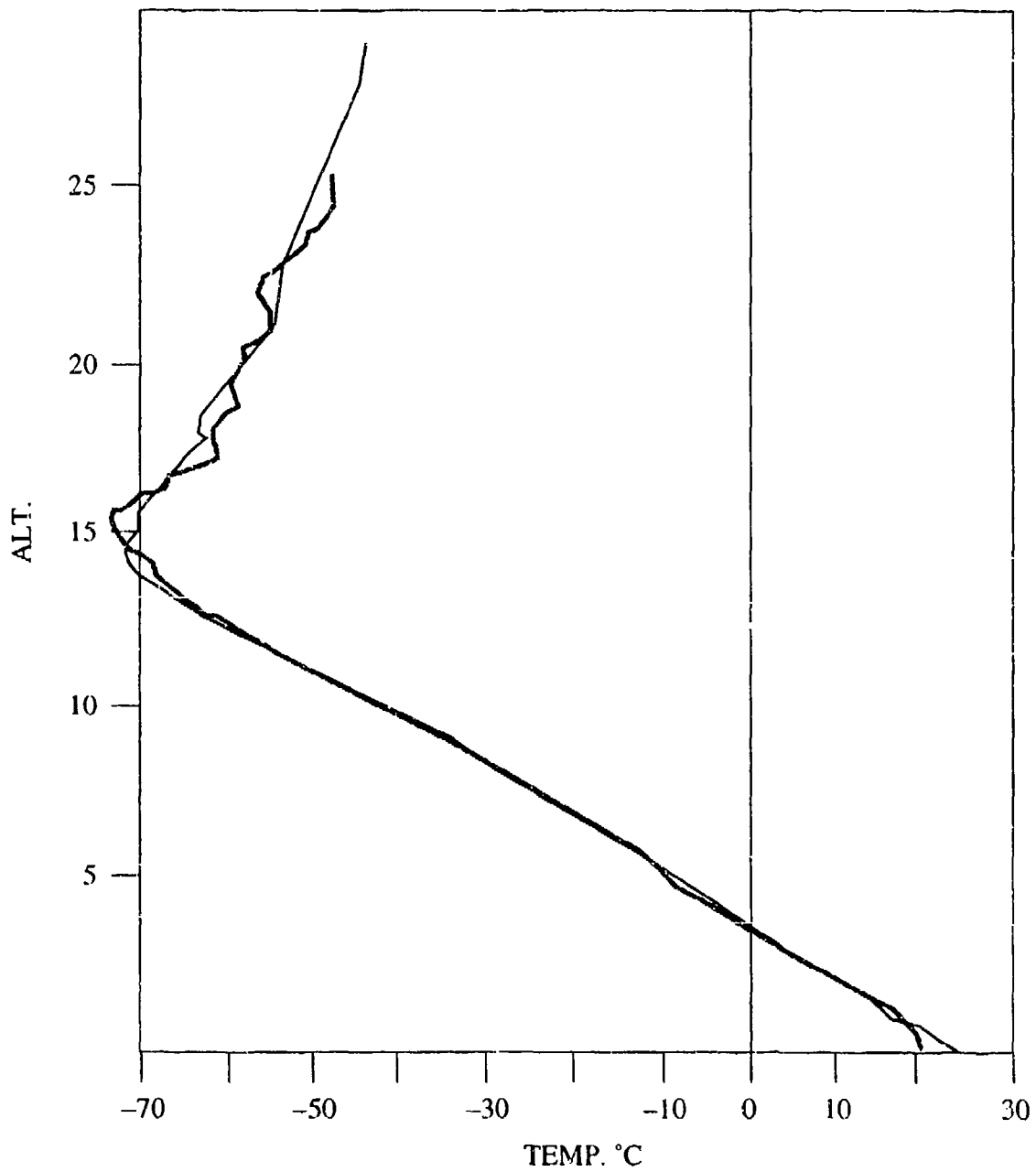
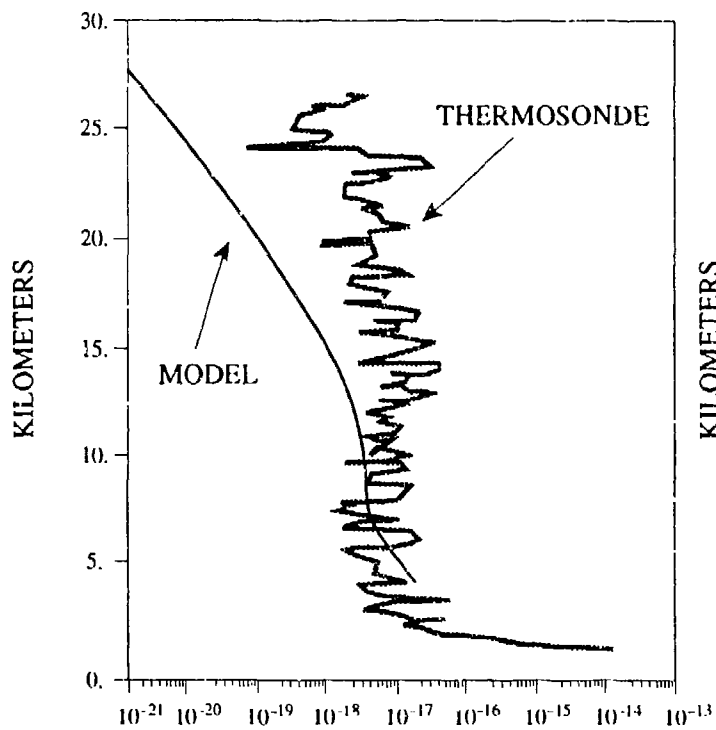
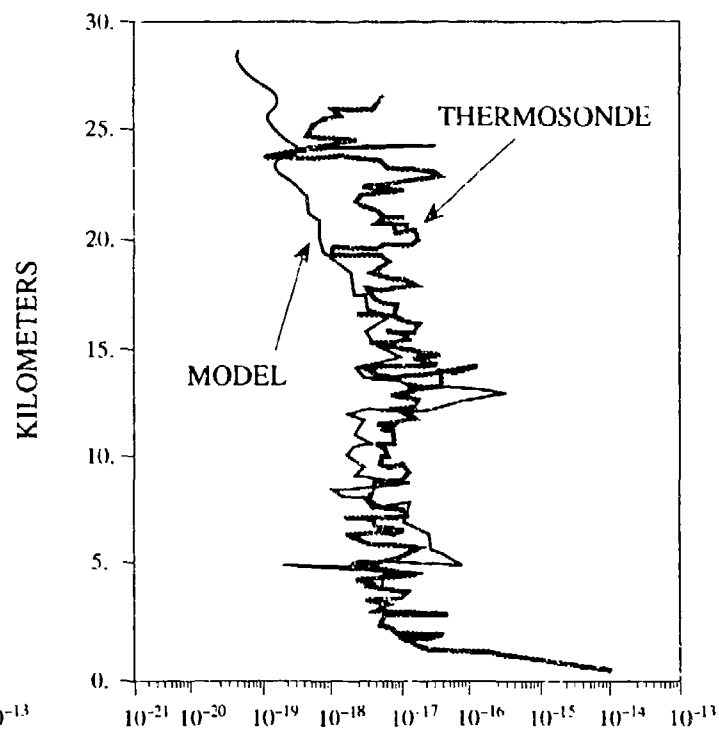


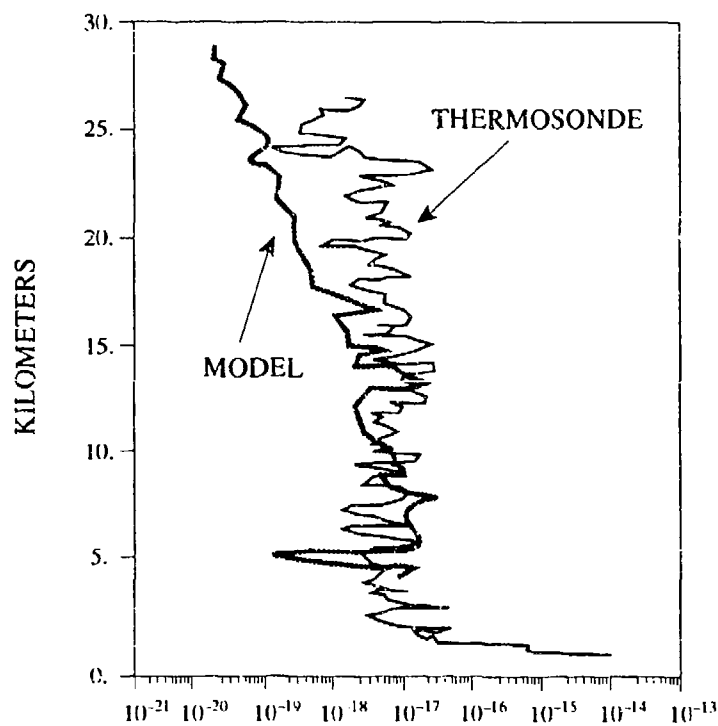
Figure A1 — Radiosonde Temperature Profile Aug 2 6am Compared to Temperature Profile From Thermosonde Balloon (the Latter Having Higher Resolution).



HUFNAGEL ESTIMATE CN••2



AFGL ESTIMATE CN••2



VAN ZANDT ESTIMATE CN••2

Figure A2 — C_N^2 Profiles: Hafnagel, Van Zandt, and AFGL models compared to thermosonde data.

Appendix B

Shear Regressions

We calculated several regressions for Y in our shear model which will now be described. Our purpose is to describe alternate models (some used in the text, and some not used) in the hope that the results might prove useful for future work.

In the text we described, in connection with Eq. (8), the technique of using an 11 point smoothing to calculate the S_{raw} values across a 300 m altitude range containing an equal range (that is, 300 m) of weight averaged length scales which gave the values of Y to plot against S_{raw} . This model was obtained for both stratosphere and troposphere. Other models involved smoothing over 29 points as well as no smoothing. All are listed in Table B1.

Table B1. Alternative Models

A. Troposphere	Constant	Slope
1. no smoothing	1.65	39.6
2. 11 pt smooth	1.64	42.0
3. 29 pt smooth	1.65	47.6
B. Stratosphere		
1. no smoothing	0.521	47.2
2. 11 pt smooth	0.506	50.0
3. 29 pt smooth	0.525	56.2

Note that increasing the smoothing has little impact upon the constant but that it increases the slope. This makes sense because, as smoothing is increased, it will reduce S_{raw} for a given value of associated $\langle \mathcal{L}^{4/3} \rangle$, the weight-averaged $\mathcal{L}^{4/3}$.

In the initial stages of our work, we employed a model (used also in Appendix A and in the CLEAR-1 study) which consisted of:

$$\begin{aligned} \text{Tropo} \quad Y &= 1.57 + 29.6 S_{raw} \\ \text{Strat} \quad Y &= 0.508 + 37.0 S_{raw} \end{aligned}$$

as mentioned in the texts (see Tables 5 and 6). This model was obtained in a calculation that involved a 150m region enclosed within the 300 m region and centrally located. It also involved a weight averaged value of \mathcal{L}_i that consisted of:

$$\langle (\mathcal{L}_i)^{4/3} \rangle = \sum (\mathcal{L}_i^{4/3} (\mathcal{L}_i / 290))$$

[compare Eq. (7) of the main text] which made no allowance for \mathcal{L}_i sections extending outside of the volume of interest. While we consider this procedure to be dubious at present, we found

that in our CLEAR-2 work (omitted in this report but contained in part in the CLEAR-2 report) the model seemed to work well. We omitted the details here because we were not sure that the CLEAR-2 velocities were reliable in unfiltered form as we used them. In any case, the text shows that performance was very close to the 11 point smooth case given in Table B1.